Published December 1, 2008

μ2 adaptin facilitates but is not essential for synaptic vesicle recycling in *Caenorhabditis elegans*

Mingyu Gu,[1] Kim Schuske,[1] Shigeki Watanabe,[1] Qiang Liu,[1] Paul Baum,[2,3] Gian Garriga,[2] and Erik M. Jorgensen[1]

[1]Howard Hughes Medical Institute and Department of Biology, University of Utah, Salt Lake City, UT 84112
[2]Department of Molecular and Cell Biology, Helen Wills Neuroscience Institute, University of California, Berkeley, Berkeley, CA 94720
[3]Division of Experimental Medicine, Department of Medicine, San Francisco General Hospital, University of California, San Francisco, San Francisco, CA 94110

Synaptic vesicles must be recycled to sustain neurotransmission, in large part via clathrin-mediated endocytosis. Clathrin is recruited to endocytic sites on the plasma membrane by the AP2 adaptor complex. The medium subunit (μ2) of AP2 binds to cargo proteins and phosphatidylinositol-4 ,5-bisphosphate on the cell surface. Here, we characterize the *apm-2* gene (also called *dpy-23*), which encodes the only μ2 subunit in the nematode *Caenorhabditis elegans*. APM-2 is highly expressed in the nervous system and is localized to synapses; yet specific loss of APM-2 in neurons does not affect locomotion. In *apm-2* mutants, clathrin is mislocalized at synapses, and synaptic vesicle numbers and evoked responses are reduced to 60 and 65%, respectively. Collectively, these data suggest AP2 μ2 facilitates but is not essential for synaptic vesicle recycling.

Introduction

After synaptic vesicle fusion, vesicle proteins are retrieved from the plasma membrane and recycled into new synaptic vesicles to sustain neuronal transmission. Recycling is thought to be initiated by the recruitment of clathrin to patches of membrane containing synaptic vesicle proteins. The reformed vesicle with a geodesic coat is budded into the cytoplasm. This model is supported by extensive associative and functional evidence. In electron micrographs of the frog neuromuscular junction, invaginating vesicles at presynaptic terminals are enveloped by a coat (Heuser and Reese, 1973). Purification of vesicles from rat brain indicate that clathrin is associated with synaptic vesicle proteins (Maycox et al., 1992). Genetic disruption of clathrin-associated endocytic proteins such as AP180, synaptojanin, dynamin, and endophilin leads to a depletion of synaptic vesicles (De Camilli et al., 1995; Nonet et al., 1999; Harris et al., 2000; Verstreken et al., 2002, 2003; Schuske et al., 2003; Newton et al., 2006). Finally, specific disruption of clathrin interactions with the adaptor protein AP180 disrupts synaptic vesicle recycling (Augustine et al., 2006; Granseth et al., 2006). These data suggest that clathrin-mediated endocytosis is the main mechanism used by synapses to recycle vesicles after exocytosis.

Clathrin is linked to cargo and membranes by the clathrin adaptor complex (Keen, 1987). Four different adaptor omplexes have been identified in mammals: AP1, AP2, AP3, and AP4 (Keen, 1987; Simpson et al., 1997; Dell'Angelica et al., 1999). These adaptor protein complexes localize to different membranes in the cell and coordinate cargo selection and vesicle biogenesis (Lewin and Mellman, 1998; Robinson and Bonifacino, 2001; Robinson, 2004). AP2 is the adaptor complex functioning during endocytosis at the plasma membrane (Mahaffey et al., 1990; Traub, 2003). There are four different subunits in the AP2 complex: α (large), β2 (large), μ2 (medium), and σ2 (small; Matsui and Kirchhausen, 1990), and each subunit serves a specific function. In particular, the μ2 subunit recruits cargo proteins containing the tyrosine-based Yxxϕ motif (Owen and Evans, 1998) and mediates in part the association of the AP2 complex to membranes (Gaidarov and Keen, 1999; Rohde et al., 2002; Honing et al., 2005).

Here, we characterize mutants that lack μ2 adaptin, encoded by the *apm-2* gene (also called *dpy-23*), in the nematode *Caenorhabditis elegans*. We demonstrate that μ2 is partially required for synaptic localization of clathrin and for the stability of the AP2 complex. However, synaptic vesicles are still recycled in the absence of μ2. Our data suggest that despite previous predictions, μ2 is not absolutely required for synaptic vesicle endocytosis. Moreover, the decrease in synaptic vesicle number

Correspondence to Erik M. Jorgensen: jorgensen@biology.utah.edu

Abbreviations used in this paper: CHC, clathrin heavy chain; ePSC, evoked postsynaptic current; mPSC, miniature postsynaptic current; ORF, open reading frame.

The online version of this article contains supplemental material.

The Rockefeller University Press $30.00
J. Cell Biol. Vol. 183 No. 5 881–892
www.jcb.org/cgi/doi/10.1083/jcb.200806088

Published December 1, 2008

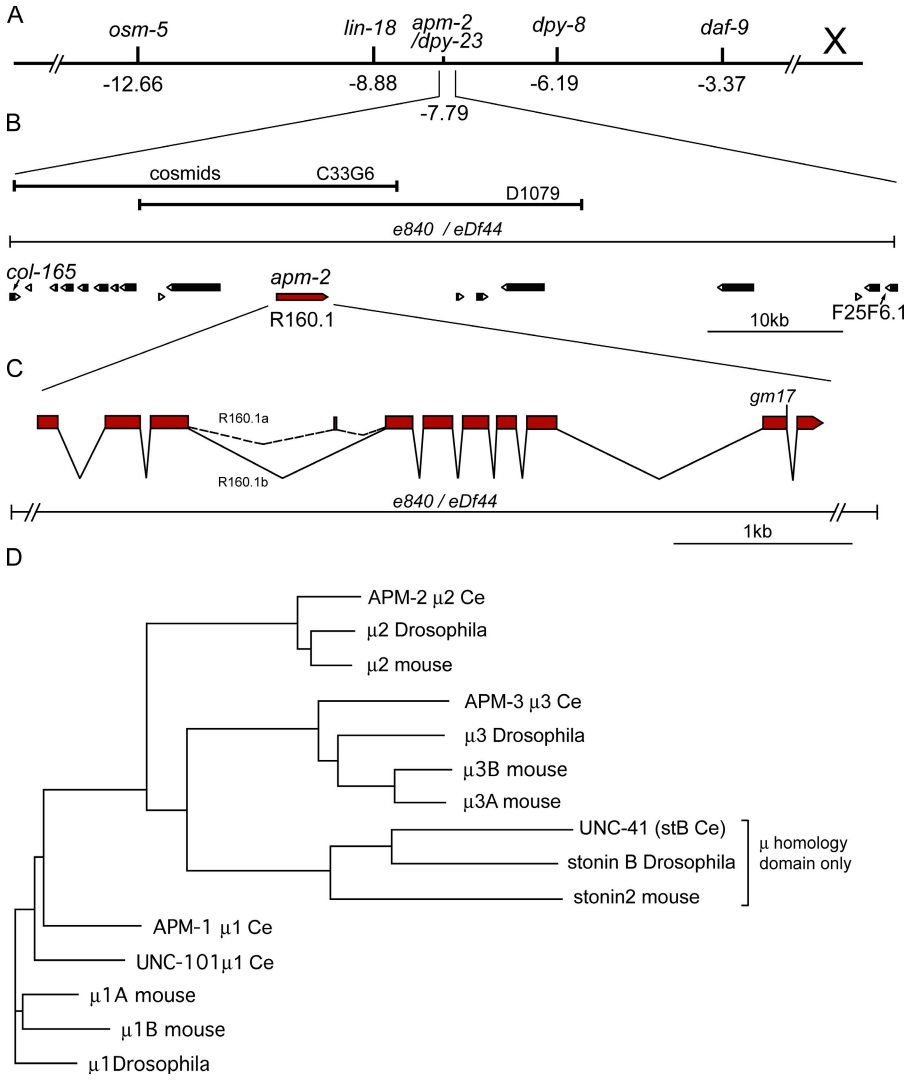

Figure 1. ***apm-2* cloning.** (A) Genetic map position of *apm-2* on chromosome X. (B) Either of two overlapping cosmids, C33G6 and D1079, rescue *apm-2(gm17)*. Below, the mutation *e840* (also called *eDf44*) is a deletion of 100 kb that removes 18 ORFs from *col-165* to F25F6.1. (C) Genomic structure of *apm-2* gene. The *e840* allele deletes the entire ORF; *gm17* is a G to A transition at the donor site of the last intron. The splice form R160.1a (Lee et al., 1994) includes an exon encoding six amino acids. This splice form is not essential because it is not required for rescue of *apm-2* mutant phenotypes (see Fig. 6 B) and is also not conserved in other species. (D) Phylogenetic tree of μ subunits from mouse, *Drosophila*, and *C. elegans*. For stonin B, only the μ homology domains were used in the alignment. See Materials and methods for accession numbers.

does not cause a locomotion defect in μ2 knockout mutants, so a smaller reserve pool might be adequate for *C. elegans* under normal condition.

Results

dpy-23/apm-2 encodes μ2 adaptin in *C. elegans*

Two mutant alleles for the locus *dpy-23 (e840* and *gm17*) have been identified. Both mutants have a variable dumpy (Dpy) phenotype in which animals vary from almost wild-type length to approximately half the size (Fig. S1 A, available at http://www.jcb.org/cgi/content/full/jcb.200806088/DC1). The dumpy phenotype is likely caused by defects in cuticle morphology. Specific defects in the cuticle are observed in the head and along the body. About 5% of the animals have "jowls" or protrusions on either side of the head (Fig. S1 B). The cuticular ridges along the body, called alae, are distorted and have multiple breaks along their length (Fig. S1 C). In addition, mutant worms are slightly uncoordinated (Unc) and have a strong egg-laying defect suggesting a role for *dpy-23* in the nervous system.

The *dpy-23* mutant phenotype was mapped to the interval between –7.91 to –7.55 on chromosome X (Fig. 1 A). The gene encoding μ2 adaptin, called *apm-2*, maps to this interval, and RNA interference to this gene gave rise to a variable dumpy phenotype suggesting *dpy-23* is likely to encode μ2 (Grant and Hirsh, 1999). We cloned the *dpy-23* gene and demonstrated that the mutated gene is *apm-2*. Two overlapping cosmids, D1079 and C33G6, in the region rescued the *dpy-23* mutant phenotype. A 12-kb genomic PCR fragment (5 kb upstream, 5 kb coding sequence of μ2 adaptin, and 2 kb downstream) could fully rescue the dumpy, uncoordinated, and egg-laying defects of *dpy-23(e840)* and *dpy-23(gm17)* (Fig. S1 A). Interestingly, overexpression of *dpy-23* in a wild-type background causes the same phenotypes as *dpy-23* loss-of-function mutations (Fig. S1 A). Because *dpy-23* encodes μ2 we will refer to the gene by its alternative name, *apm-2* (adaptor protein medium subunit 2), throughout the remainder of the manuscript.

apm-2 encodes the only μ2 subunit in *C. elegans* (Fig. 1 D). It is somewhat surprising that disruption of the single μ2 subunit in the worm gives rise to a viable animal. To determine whether μ2 adaptin is completely disrupted in the mutants, the lesions were identified. Genomic Southern analysis showed that *apm-2(e840)*

Published December 1, 2008

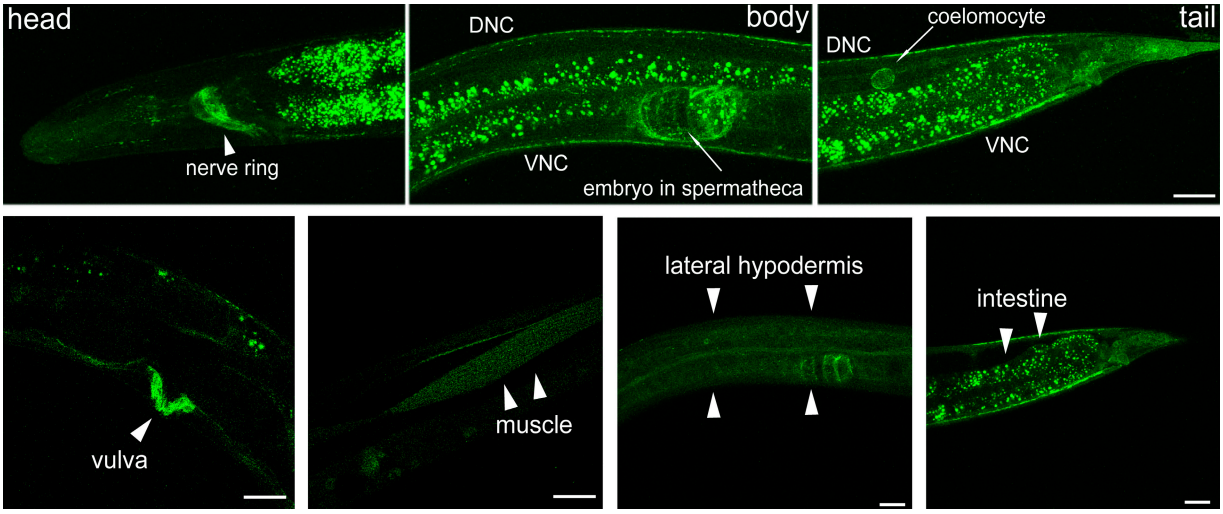

Figure 2. **APM-2 is expressed ubiquitously.** The expression pattern of translational fusion protein APM-2::GFP (Fig. S4, pMG4, available at http://www.jcb.org/cgi/content/full/jcb.200806088/DC1) in young adult hermaphrodites. Worms are oriented anterior left and dorsal up. The image of the muscle is from the transcriptional fusion of GFP driven by the *apm-2* promoter (Fig. S4, pMG3) in a young adult hermaphrodite. Muscle expression was not observed using GFP-tagged μ2, perhaps because of faint expression or synaptic localization, which overlaps strong APM-2 expression in the presynaptic terminals. The vulva and muscle expression figures are single-slice confocal images. The rest of the images are z-stack projections through the whole worm or the tissues of interest. The contrast for the image of the vulva was increased to show the outline of the worm. Bars, 20 μm. DNC, dorsal nerve cord; VNC, ventral nerve cord.

contains a deletion of ~100 kb that includes the entire coding sequence of μ2 adaptin. To identify the endpoints of the deletion, individual open reading frames (ORFs) were PCR amplified from *apm-2(e840)* mutant DNA and it was found that the deletion removes 17 additional ORFs from *col-165* to F25F6.1 (Fig. 1 B). *apm-2(gm17)* was found to contain a G to A point mutation in the splice donor site of the last intron (Fig. 1 C). Failure to splice at this intron would introduce a stop codon 27 nt downstream of the splice junction. If translated, 9 amino acids encoded by the intron would replace the 40 amino acids at the C terminus comprising β strands 15, 16, and 17. β16 has been shown to be critical for binding cargo containing the YXXϕ motif (Ohno et al., 1995; Owen and Evans, 1998). Although *apm-2(gm17)* appears to have a slightly dominant phenotype, the recessive phenotypes of *apm-2(e840)* and *apm-2(gm17)* are virtually identical, suggesting that *gm17* fully disrupts μ2 function.

μ2 is thought to be a critical component of the AP2 complex and should therefore be present in all tissues. To determine where μ2 is expressed, a construct fusing GFP to the APM-2 protein was expressed under the control of the endogenous *apm-2* promoter (Fig. S4, pMG4, available at http://www.jcb.org/cgi/content/full/jcb.200806088/DC1). Because the N terminus of μ2 adaptin is involved in assembly of the AP2 complex (Aguilar et al., 1997; Collins et al., 2002), GFP was fused to the C terminus of the APM-2 protein. The APM-2::GFP fusion protein fully rescues *apm-2* mutant phenotypes, suggesting the tagged protein is functional and is expressed in tissues that require μ2 function. Fluorescence is observed in the nervous system, coelomocyte, spermatheca, and vulva (Fig. 2). In addition, weaker expression is observed in the intestine and the hypodermis. Although fluorescence is not detected in body muscles of animals expressing the tagged protein, muscle expression is observed in animals expressing a transcriptional reporter (Fig. 2 and Fig. S4, pMG3). Thus, *apm-2* is expressed in all tissues examined, which confirms and extends a previous paper claiming that *apm-2* is expressed in neurons and some hypodermal cells (Shim and Lee, 2000).

μ2 is not essential for synaptic vesicle recycling in *C. elegans*

AP2 is thought to recruit synaptic vesicle proteins and clathrin to the endocytic zone. If μ2 is required for synaptic vesicle recycling, then several predictions can be made. First, μ2 should be localized to synapses. Second, μ2 should contribute to clathrin localization at the synapse. Third, the focus of the uncoordinated phenotype should be the nervous system. Fourth, *apm-2* mutants will have a depletion of synaptic vesicles as assayed by electron microscopy. Fifth, *apm-2* mutants will have impaired synaptic transmission as assayed by electrophysiology because of an inability to recycle vesicles.

Because *apm-2* is expressed in virtually all tissues, it is not possible to assay synaptic localization with the rescuing GFP construct, the fluorescence signal is simply too high. To look at a small subset of neurons, the *apm-2* cDNA (R160.1b) was placed under the control of a GABA neuron–specific promoter and GFP was fused at the C terminus. APM-2::GFP is localized at synapses and colocalizes with the synaptic vesicle protein synaptobrevin/VAMP (Fig. 3 A). In addition, APM-2::GFP colocalizes with C-terminal RFP-tagged clathrin heavy chain (CHC) at the synapse (Fig. 3 B). Interestingly, synaptic localization of APM-2::GFP is not dependent on AP180 (*unc-11*), synaptojanin (*unc-26*), synaptotagmin (*snt-1*), or stonin (*unc-41*) (Fig. S2 A, available at http://www.jcb.org/cgi/content/full/jcb.200806088/DC1). These data indicate that μ2 associates with synaptic varicosities as predicted, but this localization is independent of other endocytosis proteins.

Published December 1, 2008

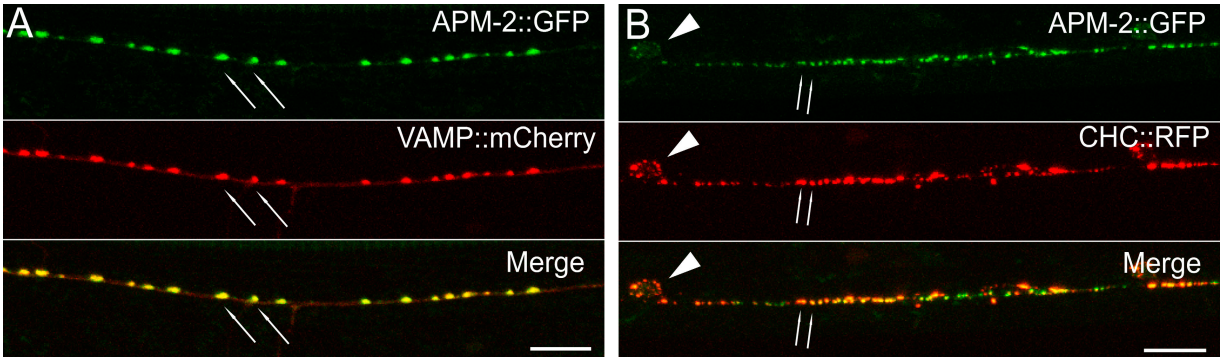

Figure 3. **APM-2 colocalizes with synaptic proteins and clathrin.** Young adult hermaphrodites were used for imaging. (A) APM-2 is localized to synapses. (top) GFP-tagged APM-2 in the GABA neuron processes in the dorsal nerve cord. (middle) mCherry-tagged synaptobrevin in the GABA neuron processes in the dorsal nerve cord. Synaptobrevin is localized to synaptic regions. The fluorescent puncta corresponds to synaptic varicosities along the dorsal muscles (arrows). (bottom) Merged image demonstrates that APM-2::GFP colocalizes with synaptobrevin at synapses. (B) APM-2 is colocalized with CHC. (top) GFP-tagged APM-2 in the GABA neuron processes in the ventral nerve cord. (middle) RFP-tagged CHC-1 in the GABA neuron processes in the ventral nerve cord. CHC is localized to both synaptic regions (arrows) and GABA neuron cell bodies (arrowhead). (bottom) Merged image demonstrates that APM-2::GFP colocalizes with CHC at synapses. Images are confocal z-stack projections through the worm nerve cord. Bars, 10 µm.

Clathrin interacts with AP2 via the appendage domain of the β2 subunit (Dell'Angelica et al., 1998). Thus, if *apm-2* mutations disrupt AP2 function, then it is possible that clathrin localization at the synapse should be altered. We analyzed the distribution of N-terminal GFP-tagged clathrin (GFP::CHC) in the dorsal and ventral nerve cords of GABA neurons in *apm-2* mutants. In the dorsal cord of *apm-2* mutants clathrin is diffuse compared with the wild type (Fig. 4; percentage of animals scored with diffuse clathrin in the dorsal cord: in the wild type, 31%, $n = 29$; in *dpy-23(e840)*, 80%, $n = 15$, $P < 0.01$; in *dpy-23(gm17)*, 70%, $n = 30$, $P < 0.01$). However, in the ventral nerve cord clathrin distribution is punctate, similar to wild-type animals (Fig. S2 B). It is possible clathrin localization near cell bodies in the ventral nerve cord is caused by AP1 function at the Golgi apparatus. Clathrin is still localized at dorsal synapses in 20–30% of the mutant animals; perhaps by other clathrin-binding proteins such as AP180, epsin, or amphiphysin. Thus, µ2 contributes to, but is not essential for, clathrin synaptic localization.

Defects in synaptic vesicle endocytosis cause the mislocalization of synaptic vesicle proteins. For example, in the absence of the endocytosis proteins, such as AP180 (Nonet et al., 1999), synaptojanin, and endophilin (Schuske et al., 2003), synaptic vesicle proteins are diffuse along the axon instead of clustering at synaptic varicosities. In contrast, the vesicle proteins synaptobrevin, synaptogyrin, and synaptotagmin are localized properly in the dorsal and lateral nerve cords of *apm-2* mutants (Fig. 4). These results suggest that µ2, unlike other endocytosis proteins, is not required to maintain vesicle proteins at the synapse.

Mutants with defects in synaptic vesicle endocytosis exhibit reduced synaptic transmission and are uncoordinated (Nonet et al., 1999; Harris et al., 2000; Schuske et al., 2003). *apm-2* mutants are also uncoordinated but the uncoordinated phenotype arises from defects in the hypodermis rather than the nervous system. When APM-2::GFP is expressed under the control of a ubiquitous promoter the tagged µ2 protein rescues all *apm-2(e840)* mutant phenotypes (Fig. 5, A and B). When µ2 protein is expressed under a pan-neuronal promoter, the *apm-2* mutants are still dumpy, uncoordinated, and egg-laying defective, effectively looking the same as the original *apm-2(e840)* mutants. In contrast, when µ2 protein is expressed under a hypodermal promoter, the *apm-2(e840)* transgenic animals are

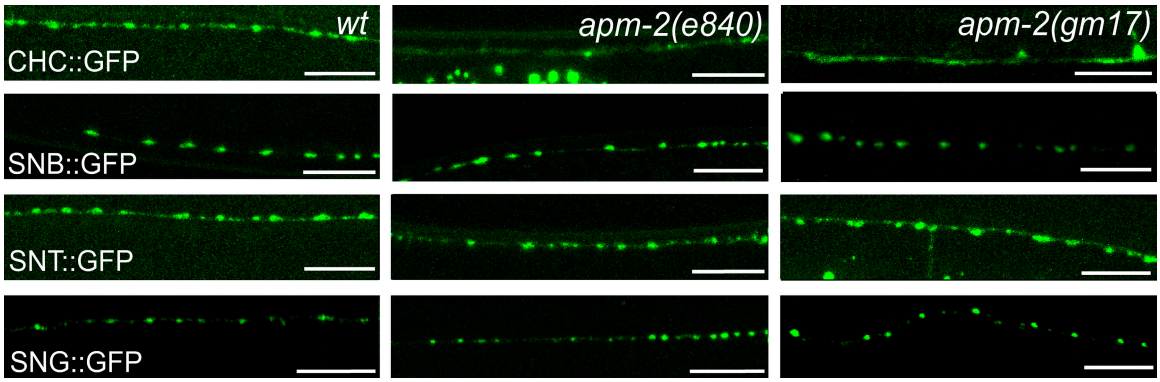

Figure 4. **Clathrin but not synaptic vesicle proteins are mislocalized in *apm-2* mutants.** For CHC, synaptobrevin (SNB), and synaptotagmin (SNT), GFP-tagged proteins were expressed in the GABA neurons and imaged in the dorsal nerve cord. Presynaptic varicosities of neuromuscular junctions along the dorsal nerve cord of an adult hermaphrodite are visible as fluorescent puncta. For synaptogyrin (SNG), GFP-tagged protein is expressed in all neurons under its own promoter and imaged in the lateral cord. Images are confocal z-stack projections through the worm nerve cord. Bars, 10 µm.

Published December 1, 2008

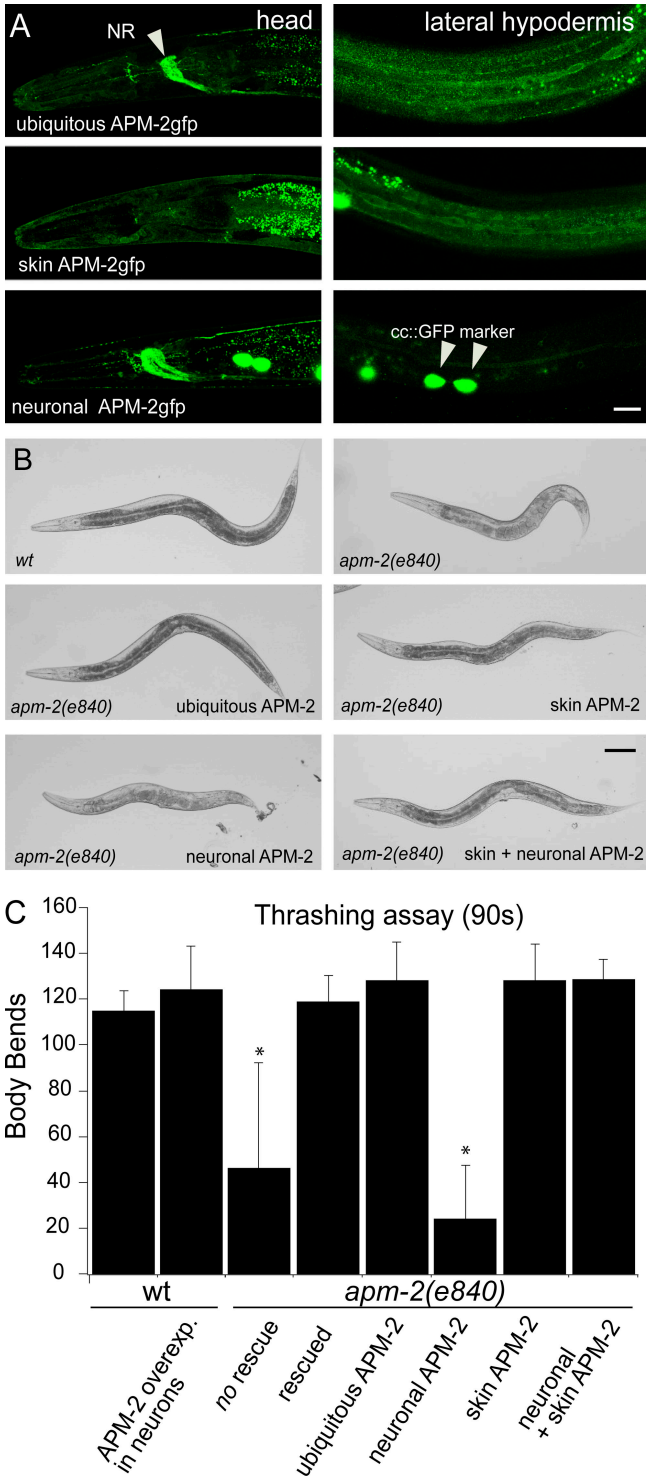

Figure 5. ***apm-2(e840)* tissue-specific rescue.** (A) APM-2::GFP expression pattern under different promoters. Ubiquitous expression is driven by the *dpy-30* promoter, hypodermal expression (skin) is driven by the *pdi-2* promoter, and neuronal expression is driven by the *rab-3* promoter (Fig S4, pMG10, pMG8, and pMG9, respectively; available at http://www.jcb.org/cgi/content/full/jcb.200806088/DC1). Worms are oriented anterior left and dorsal up. Images are confocal z-stack projections through the whole worm or the tissue of interest. All worms were imaged under identical conditions; the contrast for skin APM-2gfp panel was increased to show skin-specific expression. NR, nerve ring. Bar, 20 μm. (B) Expression of APM-2 in the skin rescues the dumpy phenotype. See Materials and methods for full genotypes. The injection concentration of *apm-2::GFP* DNA is at 1 ng/μl in all genotypes. Bar, 100 μm. (C) Thrashing assay. Expression of APM-2 in the skin rescues the locomotory phenotype. Worms were placed in buffer and body bends were counted for 90 s. Overexpression of APM-2::GFP in the nervous system (EG4017) does not create a dominant-negative phenotype (*, $P < 0.01$.). Expression of APM-2 under its own promoter (EG1616), a ubiquitous promoter (EG4015), or a skin promoter (EG4029 and EG4030) rescues thrashing. Expression of APM-2 in neurons alone does not rescue thrashing (EG4213). The data are presented as mean ± SD.

not dumpy (Fig. 5 B, skin APM-2); moreover, the jerky uncoordinated phenotype is also rescued. Previous studies have demonstrated that the μ2 functions in the skin rescue developmental defects in the nervous system (Pan et al., 2008); our data suggest that these nonautonomous defects might extend to development or function of motor neurons as well. However, skin-rescued animals are egg-laying defective and the body bends are increased in amplitude, suggesting neuronal function is somewhat altered. To quantify locomotion in the mosaic strains, animals were placed in a drop of liquid and body bends were counted for 90 s for each strain (Fig. 5 C). Thrashing rates of the hypodermal rescued strains are the same as in the wild type; whereas neuronal expression of μ2 does not rescue thrashing. The reduced thrashing is not due to a dominant-negative effect because overexpression of μ2 in the neurons does not impair locomotion in the wild type. Collectively, these data suggest the uncoordinated phenotype of *apm-2* mutants is almost exclusively caused by hypodermal defects rather than defects in the nervous system.

To directly visualize synaptic vesicles, we characterized *apm-2* mutant synapses using electron microscopy. In AP180 mutants the diameter of synaptic vesicles is increased, implicating a role for this adaptin in the control of the diameter of the reforming vesicles (Zhang et al., 1998; Nonet et al., 1999). In *apm-2(e840)* mutants, however, the diameters of synaptic vesicles are the same as in the wild type (Fig. 6 and Fig. 7 A), suggesting μ2 adaptin, unlike AP180, is not required for regulating the size of synaptic vesicles. In *apm-2(e840)* mutants, the number of remaining vesicles are 58% in acetylcholine neurons and 64% in GABA neurons compared with the wild type (Fig. 6 and Fig. 7 B). Similar vesicle reductions relative to the wild type were also observed in *apm-2(gm17)* (unpublished data). Vesicle number is rescued in *apm-2(e840)* animals containing the neuron-specific AMP-2::GFP construct but not in animals that contain the hypodermal specific APM-2::GFP, indicating that the defect is caused by a loss of neuronal APM-2 function (Fig. 6 and Fig. 7 B). The decrease in synaptic vesicle number in *apm-2* mutants suggests μ2 has a significant role in synaptic vesicle recycling. Other mutants lacking endocytosis proteins such as synaptojanin and endophilin have only 38 and 30% the normal number of vesicles, respectively (Harris et al., 2000; Schuske et al., 2003). Thus the endocytosis defect in the absence of μ2 is less severe than other endocytosis mutants. Interestingly, the reduced vesicle pool in *apm-2* mutants is able to sustain neuronal transmission because animals lacking μ2 in the nervous system are not uncoordinated. Consistent with this observation, the number of docked vesicles in *apm-2* mutants is only slightly decreased in GABA neurons and is almost normal in acetylcholine neurons (Fig. 7 C).

Published December 1, 2008

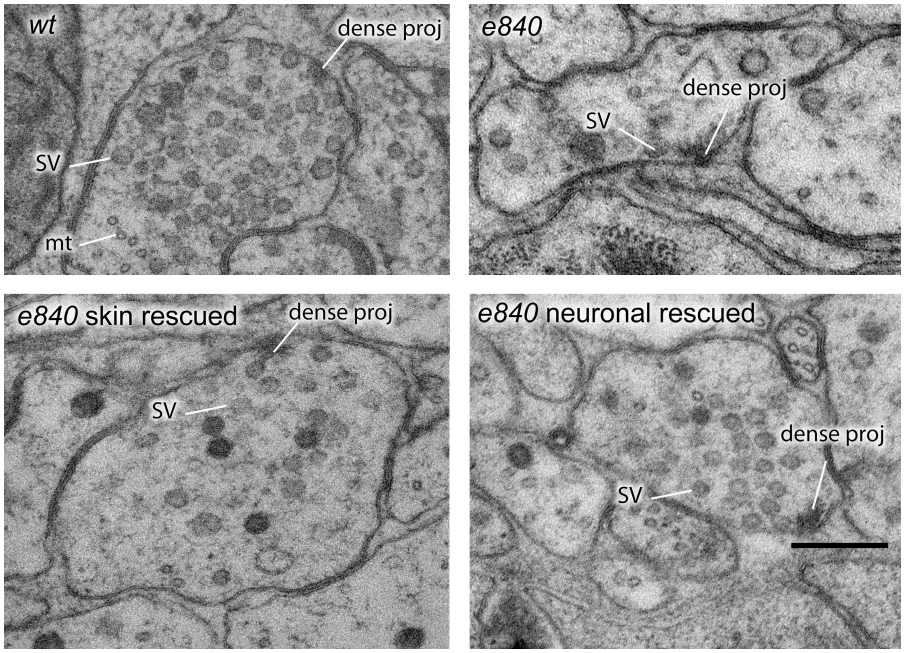

Figure 6. ***apm-2(e840)* neuromuscular junction ultrastructure.** Representative images of neuromuscular junctions in the ventral nerve cord from wild-type, EG3622 *dpy-23(e840)*, EG4029 *dpy-23(e840) Ex[Ppdi-2::APM-2::GFP]*, and EG4213 *dpy-23(e840) Ex[Prab-3::APM-2::GFP]* adult hermaphrodites. *apm-2(e840)* shows reduced numbers of synaptic vesicles. Vesicle number is restored in the neuronal-rescued animals but not in the skin-rescued animals. Bar, 200 nm. SV, synaptic vesicle; mt, microtubule; dense proj, dense projection.

To assay neurotransmitter release, animals were tested for sensitivity to the acetylcholinesterase inhibitor aldicarb (Nguyen et al., 1995). *apm-2* mutants are slightly hypersensitive to aldicarb (Fig. S3 A, available at http://www.jcb.org/cgi/content/full/jcb.200806088/DC1), and the neuronally rescued worms exhibit an identical hypersensitivity to the *apm-2* strain. Expression of *apm-2* in the hypodermis rescued the hypersensitivity to a wild-type level (Fig. S3 B), suggesting that the hypersensitivity could be caused by defects in the cuticle. To directly measure synaptic transmission, we recorded currents at neuromuscular junctions. In the *apm-2* mutants, the miniature frequency and the evoked amplitude are reduced to 60 and 82% of the wild-type levels, respectively (Fig. 8, skin rescue). These values correlate fairly well with the 55 and 69% levels of synaptic vesicles observed at GABA and acetylcholine synapses (Fig. 7 B, skin rescue). Full rescue of synaptic transmission is only observed when *apm-2* is simultaneously expressed in both the hypodermis and neurons (Fig. 8). Collectively, our data demonstrate that μ2 has a detectable role in synaptic vesicle recycling, although this role is not visible in locomotion assays.

Knocking out μ2 is not equal to knocking down AP2

Residual function from the AP2 complex could still remain in the absence of the medium subunit. There are two lines of evidence: genetic and biochemical. First, α adaptin knockdowns are more severe than μ2 adaptin knockdowns in the yolk uptake assay (Grant and Hirsh, 1999). RNA interference against clathrin, α adaptin, or β2 adaptin each abolished uptake of a GFP-tagged vitellogenin (YP170-GFP) into oocytes. In contrast, RNA interference against either μ2 or σ2 adaptin did not disrupt uptake, suggesting that not all of the subunits of the AP2 complex are required for this process. Because RNA interference is not always fully penetrant we used our deletion allele to assay μ2 function in yolk uptake. Approximately 120 gonads of each genotype were assayed for the presence of YP170-GFP fluorescence in oocytes. Over 98% of the gonads in both *apm-2(e840)* and *apm-2(gm17)* mutants were scored as positive for yolk protein uptake (Fig. 9 A). However, the number of oocytes within each gonad containing YP170-GFP was reduced in both alleles of *apm-2* compared with the wild type (wild type: one oocyte, 7%; two or more, 93%; *apm-2(e840)*: one oocyte, 42%; two or more oocytes, 58%; *apm-2(gm17)*: one oocyte, 36%; two or more oocytes, 64%; Fig. 9 B). In all genotypes yolk accumulation is greatest in the oldest oocyte, which is found adjacent to the spermatheca. The defect is not as severe as that seen when the α or β2 subunits of the complex are depleted by RNA interference (Grant and Hirsh, 1999), suggesting that μ2 adaptin subunits are less important than the α adaptin or β2 adaptin subunits in this process.

Second, some α adaptin remains in a complex with σ2 adaptin in the μ2 adaptin mutants. Previous results suggested that each subunit is required for function and stability of the AP2 complex; e.g., RNA interference of the μ2 subunit in HeLaM cells greatly reduced the expression level of the α subunit (Motley et al., 2003). In addition, expression of any single AP2 subunit in bacteria produces an insoluble protein; only simultaneous expression of all subunits produces a soluble protein complex (Collins et al., 2002). To determine if the AP2 complex is stable in the absence of the μ2 subunit, we performed quantitative Western blot analysis of α adaptin. α adaptin is reduced to 60% in *apm-2(e840)* and to 12% in *amp-2(gm17)* (Fig. 9 C). Oddly, the reduction in α adaptin is more severe in the truncated allele of μ2 rather than in the null mutant; it is possible that incorporation of truncated μ2 leads to a destabilization of the whole complex. Consistent with this result, *apm-2(e840)/+* heterozygous animals are wild type, whereas *apm-2(gm17)/+* animals are slightly uncoordinated and have an egg-laying defect. The reduction in α adaptin levels in both alleles indicates that μ2 is required to stabilize the AP2 complex; however, some residual α adaptin remains in the absence of μ2.

Supplemental Material can be found at:
http://jcb.rupress.org/cgi/content/full/jcb.200806088/DC1

Published December 1, 2008

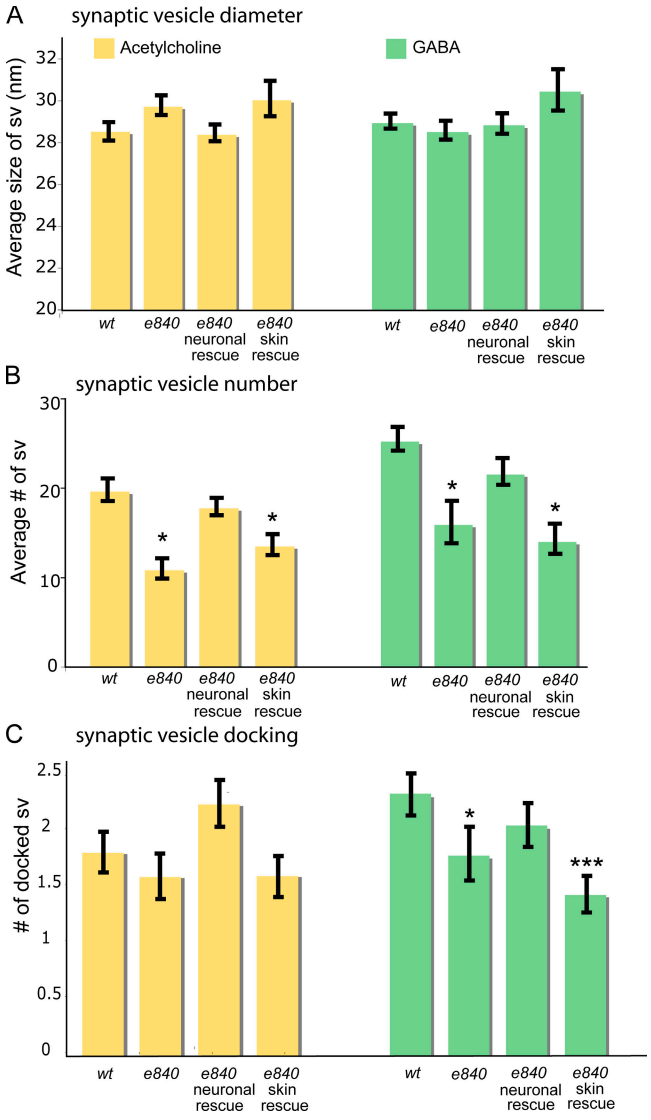

Figure 7. **Synaptic vesicle numbers are reduced in *apm-2(e840)* mutants.** The ventral nerve cord was reconstructed from serial electron micrographs and distribution of synaptic vesicles at neuromuscular junctions was measured from two young adult hermaphrodites for each genotype. (A) Vesicle diameters are identical in wild-type, *apm-2(e840)*, and *apm-2(e840)* tissue-specific rescued animals. Mean size of synaptic vesicles per profile containing a dense projection in nanometers ± SEM is as follows: wild-type acetylcholine, 28.52 ± 0.38, *n* = 734 vesicles; *apm-2(e840)* acetylcholine, 29.71 ± 0.47, *n* = 377 vesicles; neuronal-rescued *apm-2(e840)* acetylcholine, 28.38 ± 0.40, *n* = 744 vesicles; skin-rescued *apm-2(e840)* acetylcholine, 28.38 ± 0.85, *n* = 675 vesicles; wild-type GABA, 28.70 ± 0.35, *n* = 904 vesicles; *apm-2(e840)* GABA 28.27 ± 0.44, *n* = 474 vesicles; neuronal-rescued *apm-2(e840)* GABA, 28.59 ± 0.48, *n* = 1073 vesicles; skin-rescued *apm-2(e840)* GABA, 30.15 ± 0.96, *n* = 700 vesicles. (B) The number of synaptic vesicles is reduced in neurons lacking APM-2. Mean number of synaptic vesicles per profile containing a dense projection ± SEM: wild-type acetylcholine, 19.63 ± 1.28, *n* = 38 synapses; *apm-2(e840)* acetylcholine, 10.83 ± 1.13, *n* = 35 synapses; neuronal-rescued *apm-2(e840)* acetylcholine, 17.74 ± 0.97, *n* = 42 synapses; skin-rescued *apm-2(e840)* acetylcholine, 13.5 ± 1.18, *n* = 50 synapses; wild-type GABA, 25.11 ± 1.17, *n* = 36 synapses; *apm-2(e840)* GABA, 15.83 ± 2.23, *n* = 30 synapse; neuronal-rescued *apm-2(e840)* GABA, 21.46 ± 1.34, *n* = 50 synapses; skin-rescued *apm-2(e840)* GABA, 13.92 ± 1.51, *n* = 50 synapses. (C) The number of docked synaptic vesicles is slightly reduced in neurons lacking APM-2. Mean number of docked synaptic vesicles per profile containing a dense projection ± SEM: wild-type acetylcholine, 1.82 ± 0.13; *apm-2(e840)* acetylcholine, 1.60 ± 0.19; neuronal-rescued *apm-2(e840)* acetylcholine, 2.24 ± 0.20; skin-rescued *apm-2(e840)* acetylcholine, 1.60 ± 0.16; wild-type GABA, 2.36 ± 0.17; *apm-2(e840)* GABA, 1.8 ± 0.22; neuronal-rescued *apm-2(e840)* GABA, 2.06 ± 0.18; skin-rescued *apm-2(e840)* GABA, 1.44 ± 0.14. The number of synapses is the same as in B. *, P < 0.05; ***, P < 0.001.

The residual α adaptin remains bound to σ2 adaptin. α adaptin tagged with GFP was immunoprecipitated from the wild type and *apm-2* mutants. β adaptin coimmunoprecipitated from the wild-type animals but not from μ2 mutant animals (Fig. S5 A, available at http://www.jcb.org/cgi/content/full/jcb.200806088/DC1). In contrast, σ2 adaptin (HA tagged) coimmunoprecipitated from both the wild-type and μ2 mutant animals (Fig. S5, B and C). Moreover, residual α adaptin can still be localized in the absence of μ2. Coelomocytes are scavenger cells in *C. elegans* with high levels of endocytosis. N-Terminal tagged α adaptin is localized properly to the plasma membrane of mutant coelomocytes (Fig. 9 D). Similarly, tagged α adaptin is localized to synapses in *apm-2* mutants. These data suggest that the protein is folded and transported correctly in mutant cells. Thus, it is possible that AP2 is at least partially functional in *apm-2* mutants.

Discussion

In this study, we characterized the only AP2 μ2 adaptin subunit in *C. elegans* and its function in synaptic vesicle endocytosis. μ2 adaptin is encoded by the gene *dpy-23* (*apm-2*). It is expressed ubiquitously in adult worms and is highly expressed in the nervous system. Absence of μ2 impairs but does not eliminate synaptic vesicle endocytosis. Animals lacking μ2 have ∼60% of the normal number of vesicles at synaptic varicosities, and synaptic vesicle proteins are properly localized at the synapse. This phenotype is much less severe than worm mutants lacking other recycling proteins such as AP180 (*unc-11*), synaptojanin (*unc-26*), and endophilin (*unc-57*) (Nonet et al., 1999; Harris et al., 2000; Schuske et al., 2003). For example, the number of synaptic vesicles in synaptojanin and endophilin mutants is reduced to ∼35%, the normal number of synaptic vesicles found at neuromuscular junctions.

The conclusion that μ2 is not essential for synaptic vesicle recycling leads to several considerations. (a) Do other proteins recruit cargo? (b) Can other medium subunits stabilize AP2? (c) Do other proteins recruit clathrin?

The specific role of μ2 is in cargo recruitment, in particular, its interactions with synaptotagmin were thought to be essential for synaptic vesicle biogenesis (Zhang et al., 1994; Jorgensen et al., 1995; Haucke et al., 2000). However, our data indicate that μ2 is not required to recruit proteins to synaptic vesicles. The essential synaptic vesicle proteins are synaptobrevin, synaptotagmin, and the neurotransmitter transporters. Other ancillary proteins have been identified that recruit these synaptic vesicle proteins to sites of endocytosis. AP180 is required to recruit synaptobrevin to synaptic vesicles (Zhang et al., 1998; Nonet et al., 1999; Bao et al., 2005). Stonin, which is distantly related to μ2, is required for synaptotagmin recycling (Fergestad and Broadie, 2001; Martina et al., 2001; Walther et al., 2004). The vesicular GABA transporter is recruited by a

Published December 1, 2008

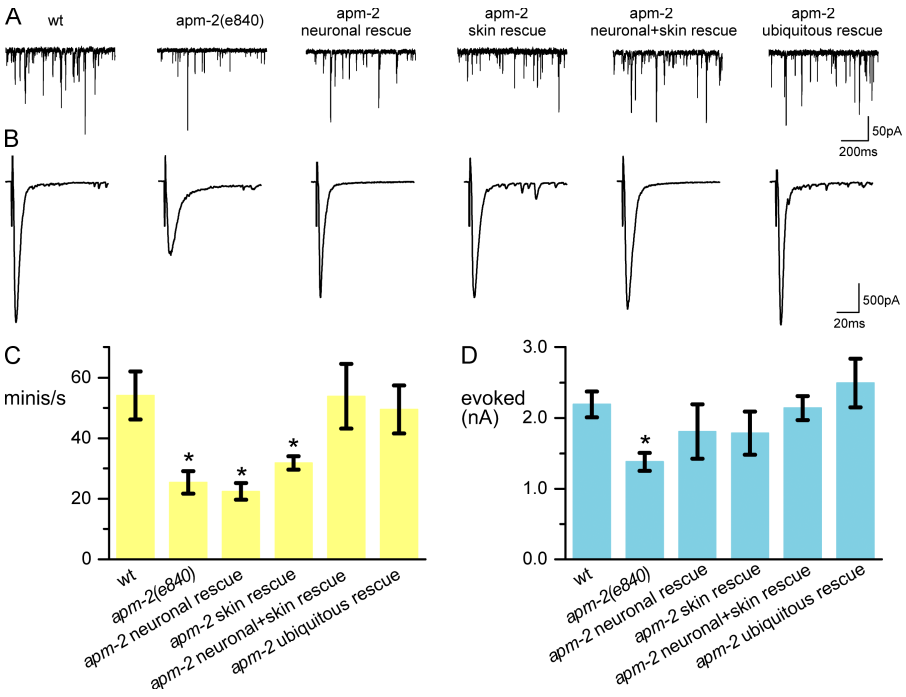

Figure 8. **Electrophysiological analysis at neuromuscular junctions of wild-type, *apm-2(e840)*, and various *apm-2(e840)* tissue-specific rescued worms.** (A) sample traces of mPSC recorded from wild-type, *apm-2(e840)*, neuronal-rescued *apm-2(e840)*, skin-rescued *apm-2(e840)*, neuronal- and skin-rescued *apm-2(e840)*, and ubiquitously rescued *apm-2(e840)* worms. (B) sample traces of ePSC recorded from the aforementioned animals. (C) Summary of mPSC frequencies (Hz ± SEM): wild type, 54.1 ± 8.0, n = 8; *apm-2(e840,)* 25.4 ± 3.7, n = 9; neuronal-rescued *apm-2(e840)*, 22.4 ± 2.7, n = 8; skin-rescued *apm-2(e840)*, 31.9 ± 2.2, n = 12; neuronal- and skin-rescued *apm-2(e840)*, 53.9 ± 10.7, n = 8; ubiquitously rescued *apm-2(e840)*, 49.5 ± 7.9, n = 8. (D) Summary of ePSC amplitudes (nA ± SEM): wild type, 2.19 ± 0.18, n = 8; *apm-2(e840)*, 1.38 ± 0.13, n = 7; neuronal-rescued *apm-2(e840)*, 1.81 ± 0.39, n = 7; skin-rescued *apm-2(e840)*, 1.79 ± 0.31, n = 8; neuronal- and skin-rescued *apm-2(e840)*, 2.14 ± 0.17, n = 6; ubiquitously rescued *apm-2(e840)*, 2.50 ± 0.34, n = 7. *, $P < 0.05$, compared with wild-type; unpaired t test.

LAMP-related protein called UNC-46 (Schuske et al., 2007). Because of these defects in cargo recruitment, all of these mutants are severely uncoordinated in worms. In contrast, mutants lacking μ2 in the nervous system are not uncoordinated and evoked responses are at 82% of the levels observed in the wild type, indicating that synaptic transmission is largely intact. Thus, if μ2 recruits cargo to recycling vesicles it is unlikely to be a component essential for neurotransmission.

The medium subunit μ2 is also known to stabilize the AP2 complex (Motley et al., 2003). One could imagine that medium subunits from the AP1 or AP3 complexes (there is no AP4 in *C. elegans*) could substitute for μ2 and provide AP2 complex function. However, adaptins from different complexes do not appear to be redundant in other organisms. For example, in yeast, overexpression of σ2 cannot substitute for the loss of σ1 (Phan et al., 1994). Similarly, we found that other medium subunits cannot substitute for μ2 in *C. elegans*. Mutants lacking μ1 (*unc-101*) are severely uncoordinated and exhibit defects in anterograde transport of olfactory receptors to olfactory cilia (Dwyer et al., 2001). Overexpression of μ2 cannot rescue the severely uncoordinated phenotype of the μ1 mutant in a thrashing assay (unpublished data). Moreover, *apm-2 unc-101* (μ1 μ2) double mutants exhibit an additive dumpy and uncoordinated phenotype rather than a synthetic phenotype, suggesting that these proteins are not acting redundantly. Mutants lacking μ3 (*apm-2(tm920)*) are outwardly wild type but slightly aldicarb resistant. Again, μ2 and μ3 mutations do not show synthetic interactions: *apm-2 apm-3* double mutants (with μ2 rescued in skin) exhibit similar aldicarb sensitivity as the μ3 mutant alone. In addition, our data show that AP2 is destabilized in the absence of μ2, suggesting μ2 is the only medium subunit used by AP2 in *C. elegans*.

Our data are consistent with a study in other systems suggesting that clathrin can be recruited by alternative adaptors (Traub, 2003). In particular, AP180 is required for normal synaptic vesicle endocytosis and it is likely that AP180 could recruit clathrin and form vesicles in the absence of AP2 (Zhang et al., 1998; Nonet et al., 1999). Our results for μ2 seem to conflict with previous studies that suggest that the AP2 subunit α adaptin is essential for synaptic vesicle recycling in *Drosophila melanogaster*. A weak mutation in the *Drosophila* α adaptin subunit *D-αAda*^{1} leads to slowly moving larvae, which die as pupae (Gonzalez-Gaitan and Jackle, 1997). The neurons of these animals are not efficient in taking up FM1-43 dye at boutons upon stimulation. The null mutants die before hatching and the electron microscopy data suggest that these animals are depleted of synaptic vesicles. However, in *C. elegans*, the behavioral defects of *apm-2*–null mutants are less pronounced. The hypodermal rescued mutants have almost normal movement and the evoked current upon stimulation is close to the wild type. Thus the neurotransmission defect in μ2 mutants in worms is less severe than that of α adaptin mutants in flies. Although it is possible that residual AP2 function accounts for vesicle recycling in μ2 mutants, it is also possible that AP2 is not essential for synaptic vesicle recycling at *C. elegans* neuromuscular junctions.

Materials and methods

Mapping and mutation analysis

The mutation *e840* was isolated in an x-ray mutagenesis by S. Brenner (Agency for Science, Technology, and Research, Biopolis, Singapore). The mutation *gm17* was isolated in an EMS screen for egg-laying defective animals. *gm17* was mapped between two polymorphisms on the X chromosome, *gmP'* and *pgP2*, and was successfully rescued by two overlapping cosmids, D1079 and C33G6. The sequence of *gm17* was determined by DNA sequencing. The molecular nature of *e840* was determined by genomic southern analysis and the break points of *e840* deletion were further characterized by PCR against *apm-2* neighboring ORFs. Because *e840* is a multigene deletion, an alternative name, *eDf44*, has been given by J. Hodgkin (University of Oxford, Oxford, England).

Published December 1, 2008

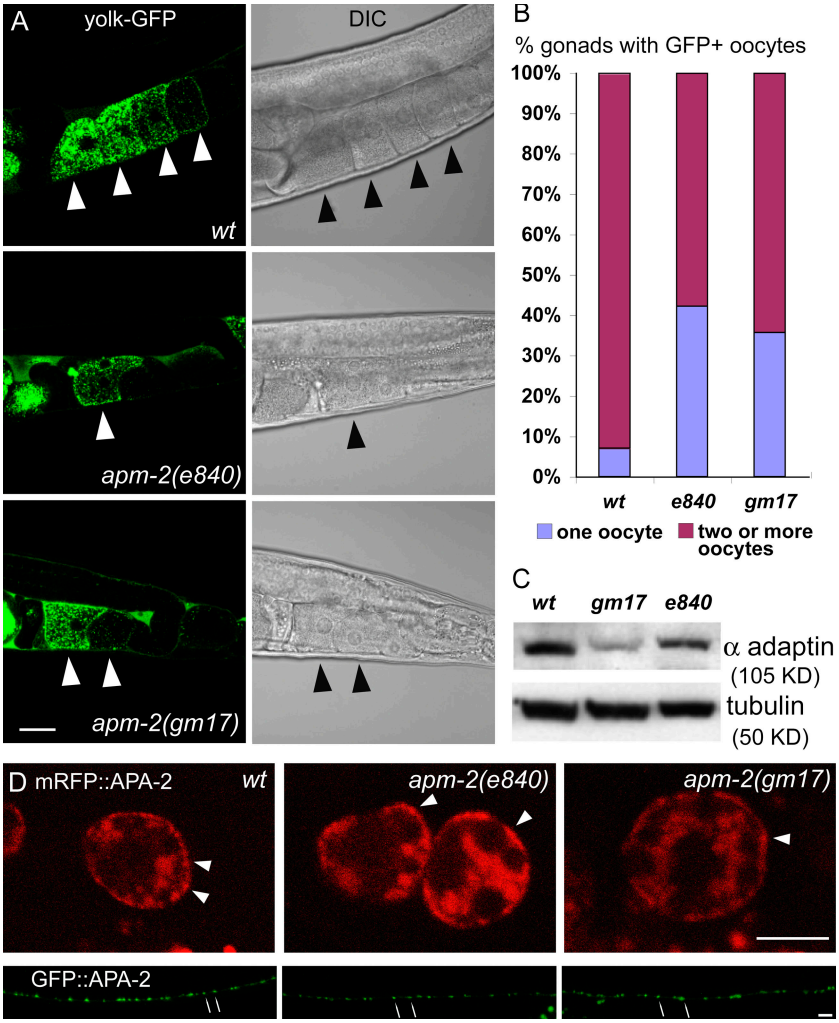

Figure 9. **Yolk protein endocytosis in *apm-2* mutants.** (A) Oocytes from adult worms expressing yolk protein YP170::GFP. Arrowheads indicate the GFP-positive oocytes. Figures are single-slice confocal images. Bar, 20 μm. (B) A bar graph showing the percentage of gonads with different numbers of GFP-positive oocytes. (C) A Western blot of the wild-type and *apm-2* mutant worm lysates probed with an antibody against α adaptin (APA-2). 200 μg of protein was loaded in each lane. (D) APA-2 localization in scavenger cell, coelomocytes, and GABA synapses. Images were taken from adult worms. Arrowheads indicate the RFP-positive plasma membrane of coelomocytes. Arrows indicate the GFP-positive synapses. Coelomocyte figures are single-slice confocal images. GABA synapse images are z-stack projections. Bars, 5 μm.

C. elegans strains

The wild strain is Bristol N2. The reference strains for *e840* and *gm17* were outcrossed twice before phenotypic analysis. The outcrossed strains are EG2988 *apm-2(gm17)X* and EG3622 *apm-2(e840)X*.

The strains used in the synaptobrevin and clathrin colocalization assays were EG4052 *lin-15(n765ts)X; oxEx761[Punc-47:APM-2(cDNA)::GFP Punc-47:SNB::mCherry lin-15(+)]* and EG4051 *lin-15(n765ts)X; oxEx759[Punc-47:APM-2(cDNA)::GFP Punc-47:CHC-1::RFP lin-15(+)]*.

The strains used in the synaptic vesicle protein distribution assays were MT8247 *lin-15(n765ts) nIs52[Punc-25::SNB::GFP lin-15(+)]X*, EG3733 *apm-2(e840) nIs52[Punc-25::SNB::GFP lin-15(+)]X*, EG3229 *apm-2(gm17) nIs52[Punc-25::SNB::GFP lin-15(+)]X*, NM1233 *jsIs219[SNG-1::GFP rol-6(su1006)]II*, EG3563 *jsIs219[SNG-1::GFP rol-6(su1006)]II; apm-2(e840)X*, EG3736 *jsIs219[SNG-1::GFP rol-6(su1006)]II; apm-2(gm17)X*, EG3855 *lin-15(n765ts) oxIs224[Punc-47::GFP::SNT-1 lin-15(+)]X*, EG3889 *apm-2(e840) oxIs224[Punc-47::GFP::SNT-1,lin-15(+)]X*, and EG3891 *apm-2(gm17) oxIs224[Punc-47:GFP::SNT-1 lin-15(+)]X*.

The strains used in the clathrin distribution assays were EG3381 *oxIs-164[Punc-47::GFP::CHC-1 lin-15(+)]IV; lin-15(n765)X*, EG3735 *oxIs-164[Punc-47:GFP::CHC-1 lin-15(+)]IV; apm-2(e840)X* and EG3564 *oxIs164[Punc-47::GFP::CHC-1 lin-15(+)]IV; apm-2(gm17)X*.

The strains used in APM-2 distribution assays were EG4055 *snt-1(n2665)II; oxEx763[Punc-47::APM-2(cDNA)::GFP Pmyo-2::GFP]*, EG4091 *unc-41(n268)V; oxEx767[Punc-47::APm-2(cDNA)::GFP Pmyo-2::GFP]*, EG4103 *unc-11(e47)I; oxEx767[Punc-47::APM-2(cDNA)::GFP Pmyo-2::GFP]*, and EG4089 *unc-26(s1710)IV; oxEx767[Punc-47::APM-2(cDNA)::GFP Pmyo-2::GFP]*.

The strains used in APM-2 tissue-specific rescue assay were EG4017 *lin-15(n765)X; oxEx747[Prab-3::APM-2(cDNA)::GFP (pMG9) lin-15(+)]*, EG1616 *apm-2(e840)X; oxEx730[APM-2::GFP (pMG4) Punc-122::GFP]*, EG4213 *apm-2(e840)X; oxEx789[Prab-3::APM-2(cDNA)::GFP (pMG9) Punc-122::GFP]*, EG4015 *apm-2(e840)X; oxEx745[Pdpy-30::APM-2(cDNA)::GFP (pMG10) Punc-122::GFP]*, EG4029 *apm-2(e840)X; oxEx753[Ppdi-2::APM-2(cDNA)::GFP (pMG8) Punc-122::GFP]*, EG4030 *apm-2(e840)X; oxEx745[Ppdi-2::APM-2(cDNA)::GFP (pMG8) Prab-3::APM-2(cDNA)::GFP (pMG9) Punc-122::GFP]*, and EG4093 *apm-2(e840)X, oxEx773[Ppdi-2::APM-2(cDNA)::GFP (pMG8) Pmyo-2::GFP]*. *Punc-122* is the coelomocyte promoter.

The strains used in yolk uptake assay were DH1033 *sqt-1(sc103)II; bIs1[[vit-2::GFP rol-6(su1006)]X*, EG4062 *apm-2(e840) bIs1[vit-2::GFP rol-6(su1006)]X*, EG4059 *apm-2(gm17) bIs1[vit-2::GFP rol-6(su1006)]X*.

The strain used in α adaptin coelomocyte plasma membrane localization assay were RT490 *unc-119(ed3) III; pwIs177[Punc-122:mRFP::apa-2; cb-unc-119(+)]*, EG4188 *apm-2(e840) X; pwIs177[Punc-122:mRFP::apa-2; cb-unc-119(+)]*, EG4189 *apm-2(gm17) X; pwIs177[Punc-122:mRFP::apa-2; cb-unc-119(+)]*. They were provided by B.D. Grant (Rutgers University, Piscataway, NJ)

The strains used in α adaptin GABA synaptic localization assay were GK275 *unc-119(ed3) III; dkIs160[Punc-25:GFP::apa-2,unc-119(+)]*, EG4203 *apm-2(e840) X; dkIs160[Punc-25:GFP::apa-2,unc-119(+)]*, and EG4204 *apm-2(gm17) X; dkIs160[Punc-25:GFP::apa-2,unc-119(+)]*. They were provided by K. Sato (Gunma University, Gunma, Japan).

The strains used in AP2 assembly immunoprecipitation were EG5264 *oxEx1275[Papa-2::apa-2::GFP Punc-122::GFP]*, EG5265 *apm-2(e840)X, oxEx1275[Papa-2::apa-2::GFP Punc-122::GFP]*, EG5266 *oxEx1276[Papa-2::apa-2::GFP Paps-2::aps-2::HA Punc-122::GFP]*, and EG5267 *apa-2(e840)X oxEx1276 [Papa-2::apa-2::GFP Paps-2::aps-2::HA Punc-122::GFP]*.

Phylogenetic analysis

The phylogenetic tree of μ adaptin was made by ClustalX (1.83.1 Mac) and Treeview X. The protein accession numbers are as follows: μ3A mouse (Q9JKC8); μ3B mouse (Q8R2R9); μ3 *Drosophila* (NP_788873); APM-3

(NP_508184); stB *Drosophila* (Q24212); APT-10 (stB Ce; NP_505566); stB mouse (NP_780576); μ2 *Drosophila* (NP_732744); μ2 mouse (NP_033809); APM-2 (NP_001024865); APM-1(NP_491572); UNC-101 (NP_001040675); μ1A mouse (AAF61814); μ1B mouse (AF067146); μ1 *Drosophila* (NP_649906).

GFP constructs

pMG1, *apm-2* genomic region. A 12-kb *apm-2* genomic PCR fragment was amplified from cosmid C33G6, including 5 kb upstream of the start codon, 5 kb of coding sequence, and 2 kb downstream of the stop codon, and was cloned between BamHI and PstI restriction sites in pGEM-3zf(+) (Promega). Primers used were 5′-ATTAGGATCCAGGTGGTGGTGGTGAAGA-3′ and 5′-AGATCTGCAGTCGGCTAACGGCTAATTCGGCTAA-3′.

pMG2, *apm-2* transcriptional GFP. The construct comprises the *apm-2* promoter only driving GFP. This construct does not show expression in neurons, suggesting that a neuronal enhancer is contained within an intron.

pMG3, *apm-2* transcriptional GFP. GFP with the *unc-54* 3′UTR was PCR amplified from the plasmid pPD95.77 (provided by A. Fire, Carnegie Institution of Washington, Baltimore, MD). The primers used were 5′-GGCTGAAATCACTCACAACGATGG-3′ and 5′-TACAGTCGACTACGGCCGACTAGTAGGAAACAGT-3′. This fragment contains SalI restriction sites at both ends and was inserted into the SalI site of pMG1, which is in the second exon of *apm-2*.

pMG4, *apm-2* translational GFP. *apm-2* 10-kb genomic PCR fragment, including 5 kb upstream of the start codon and 5 kb of coding sequence without the stop codon, was amplified from pMG1 and cloned between the BamHI and PstI restriction sites in pGEM-3zf(+). Primers used were 5′-ATTAGGATCCAGGTGGTGGTGGTGAAGA-3′ and 5′-ACAGCTGCAGGCATCTGGTTTCATACAGTCCCGA-3′. GFP with the *unc-54* 3′UTR was cloned from the plasmid pPD95.77 with a PstI site at one end and a HindIII site at the other end and was then inserted after the *apm-2* coding sequence to make a GFP fusion protein. Primers used were 5′-ACATCTGCAGTTGGCCAAAGGACCCAAAGGTATG-3′ and 5′-ACGCAAGCTTCGGCCGACTAGTAGGAAACAGTTA-3′.

Constructs for *apm-2* tissue-specific rescue assay

Multisite Gateway three-fragment construction vectors were used (Invitrogen). Promoter entry vectors, including pENTRY4-1 *Pdpy-30* and pENTRY4-1 *Ppdi-2*, were ordered from Open Biosystems. The *Ppdi-2* construct (Open Biosystems) lacks 373 nt (−808 to approximately −435 from the start codon of *pdi-2*) in the promoter region; however, skin expression was still observed using this construct. pENTRY4-1 *Prab-3* was generated by BP reaction. ORF entry vector pENTRY1-2 *apm-2* (ORF) was ordered from Open Biosystems. 3′UTR entry vector pENTRY2-3 GFP::*unc-54* 3′UTR was made by a Gateway BP reaction. The final constructs, *apm-2*::GFP fusion gene driven by different promoters, were generated by Gateway LR reactions.

Constructs for AP2: assembly immunoprecipitation

pMG16, *apa-2* translational GFP. *apa-2* 6-kb genomic sequence, including 2.3 kb of promoter and 3.7 kb of coding sequence without stop codon, was cloned between KpnI and XbaI sites in pGEM-3zf(+). Primers used were 5′-ACTCGGTACCGCATACTTGATGGAAAACCCGCTC-3′ and 5′-AGCCTCTAGAAAATTGGTTGCCCAATAAGTCTAC-3′.

GFP with the *unc-54* 3′UTR was cloned from Fire laboratory vector pPD 95.77 with an XbaI site at one end and a HindIII site at the other end. This fragment was inserted after the *apm-2* coding sequence to make a GFP fusion protein. Primers used were 5′-ACCGTCTAGAGGGGTAGAAAAATGAGTAAAGGA-3′ and 5′-AGCGAAGCTTCGGCCGACTAGTAGGAAACAGTTA-3′.

pMG28, HA-tagged translational APS-2. *aps-2* 2-kb genomic sequence, including 1 kb of promoter and 1 kb of coding sequence (stop codon is replaced by HA tag), was cloned between EcoRI and PstI sites in pGEM-3zf(+). Primers used were 5′-AGCGGAATTCCGTTTAGTTCTTGAGTGGCTTG-3′ and 5′-ACAGCTGCAGAGCGTAATCTGGAACATCGTATGGGTATTCCAGGGAAGTAAGCATGAGCA-3′.

unc-54 3′UTR was cloned from Fire laboratory vector pPD 95.77 with a PstI site at one end and a HindIII site at the other end. This fragment was inserted after the *aps-2::HA* coding sequence. Primers used were 5′-AGGCCTGCAGTAGCATTCGTAGAATTCCAACTGA-3′ and 5′-AGGCAAGCTTCCCATAGACACTACTCCACTTTC-3′.

Microinjection

The total DNA concentration of injection mix is 100 ng/μl. The injection marker was 50 ng/μl *Punc-122::GFP*, if not specified. 1-kb DNA ladder (Fermentas) was used to make the injection mix final concentration 100 ng/μl.

Rescue experiment. 10 ng/μl of 12-kb *apm-2* genomic PCR fragment was injected into N2 to overexpress APM-2 in wild-type animals. 0.25 ng/μ of 12-kb *apm-2* genomic PCR fragment was injected into N2. The extrachromosomal array was then crossed into *apm-2(e840)* and *apm-2(gm17)* mutants to evaluate rescue.

Tissue-specific rescue. 1 ng/μl each of pMG10 *Pdpy-30::apm-2::GFP*, pMG8 *Ppdi-2::apm-2::GFP*, and pMG9 *Prab-3::apm-2::GFP* DNAs were injected, respectively, into *apm-2(e840)*. For the skin and nervous system double rescue experiment, 1 ng/μl each of pMG8 and pMG9 were injected together. 10 ng/μl pMG9 and 50 ng/μl *lin-15(+)* were coinjected into *lin-15(n765ts)* to overexpress APM-2::GFP only in the nervous system. 1 ng/μl pMG8 and 2 ng/μl *Pmyo-2::GFP* were coinjected into *apm-2(e840)* to rescue *apm-2* mutant in skin with a different injection marker.

AP2 complex immunoprecipitation. pMG16 was injected at 10 ng/μl into the wild type. The array was crossed into *apm-2(e840)*. pMG16 and pMG28 were coinjected at 10 ng/μl into the wild type and the same array was then crossed into *apm-2(e840)*.

Western blot analysis

Worm samples were prepared by boiling 1 vol of the worm pellet in 9 vol of 1× loading buffer for 5 min. Samples were run on a 10% SDS-PAGE gel then transferred to polyvinylidene fluoride transfer membrane (Immobilon). Primary antibody for α adaptin was a rabbit polyclonal APA-2 antibody at a dilution of 1:500 (provided by B. Grant). Primary antibody incubation was done in 1% milk at room temperature for 4 h. Primary antibody for the standard control tubulin was a 12G10 mouse monoclonal antibody (Developmental Studies Hybridoma Bank) at a dilution of 1:5,000. Primary antibody incubation was done in 1% milk at room temperature for 1 h, and then the membrane was washed three times in 10 ml of 1× PBS plus Tween 20 (PBST). Secondary antibodies were anti-rabbit and mouse IgG fragment conjugated with HRP (GE Healthcare). Secondary incubations were done in 10% milk at room temperature for 45 min, and then the membrane was washed five times in 10 ml of 1× PBST. Detection reagent used was Lumigen PS-3 (GE Healthcare).

AP2 complex immunoprecipitation

250 μl (± 50 μl) of worm pellet was harvested. The pellet was suspended in 2 ml of ice-cold lysis buffer (5% Triton X-100, 50 mM Hepes, pH 7.3, 50 mM NaCl, and 1 tablet of protease inhibitor cocktail [Roche]). The sample was lysed by a bead beater (NMB) for 10 s, three times, and was spun, and the supernatant was recovered. The supernatant was pushed through a 0.22-μm filter. 15 μl of agarose-conjugated rat anti-GFP IgG2a beads (MBL International) were added to the lysate. The mixture was incubated at 4°C for 2 h. Beads were harvested and washed with 1 ml of lysis buffer three times. 100 μl of loading buffer was added on the bead pellet and boiled for 15 min.

Samples were run on 7, 10, or 15% SDS-PAGE and transferred to a polyvinylidene fluoride membrane. Primary antibody for GFP was a mouse monoclonal antibody at a dilution of 1:5,000 (Clontech Laboratories, Inc.). Primary antibody for HA was a mouse monoclonal antibody (12CA5; Santa Cruz Biotechnology, Inc.) at a dilution of 1:5,000. Primary antibody for β adaptin was a mouse monoclonal antibody (Thermo Fisher Scientific) at a dilution of 1:5,000. Primary antibody incubation was performed in 5% BSA at 4°C overnight, and then the membrane was washed three times in 10 ml of 1× PBST. Secondary antibodies were goat anti–mouse IgG fragment conjugated with HRP (GE Healthcare). Secondary incubations were performed in 5% BSA at 22.5°C for 2 h, and then the membrane was washed five times in 10 ml of 1× PBST. Detection reagent was SuperSignal West Dura kit (Thermo Fisher Scientific).

Thrashing assay

A single worm was put into a 50-μl drop of M9 solution. The worm was allowed to adapt to the liquid environment for 2 min. The number of body bends was counted for 90 s for each genotype ($n = 7$). We analyzed lines of *apm-2(e840)* rescued by skin APM-2::GFP with two different injection markers (EG4029 *Punc-122::GFP* and EG4093 *Pmyo-2::GFP*). The results are the same.

Aldicarb resistance assay

Each agar plate was seeded with bacteria and weighed to top spread plates with the appropriate amount of aldicarb. Plates with six different aldicarb final concentrations were prepared (0.1, 0.3, 0.5, 0.7, 0.9, and 1.1 mM). Aldicarb was allowed to soak in overnight at room temperature.

For each genotype, 20 worms were put onto plates containing each different aldicarb concentration. The plates were blinded and the percentage of paralyzed worms were scored after 4 h of exposure to aldicarb. The same experiment was repeated five times for each genotype except *apm-2(e840) oxEx755[Prab-3::apm-2::GFP, Punc-122::GFP]*, which had only 10 worms on each plate and the experiment was repeated four times because of fewer transgenic animals.

Confocal microscopy

Worms are immobilized by using 2% phenoxy propanol and imaged on a confocal microscope (Pascal LSM5; Carl Zeiss, Inc.) with a plan-Neofluar 10x 0.3 NA, 20x 0.5 NA, or 40x 1.3 NA or plan-apochromat 63x 1.4 NA oil objectives (Carl Zeiss, Inc.).

Electron microscopy

Wild-type (N2), *apm-2(e840)*, EG4029 *apm-2(e840); oxEx753[Ppdi-2::apm-2::GFP, Punc-122::GFP]*, and EG4213 *apm-2(e840); oxEx789[Prab-3::apm-2::GFP, Punc-122::GFP]* adult nematodes were prepared in parallel for transmission electron microscopy as previously described (Hammarlund et al., 2007). In brief, 10 young adult hermaphrodites were placed onto a freeze chamber (100-µm well of type A specimen carrier) containing space-filling bacteria, covered with a type B specimen carrier flat side down, and frozen instantaneously in the HPM 010 (Leica). This step was repeated for animals of all genotypes. The frozen animals were fixed in the EM AFS system (Leica) with 1% osmium tetroxide and 0.1% uranyl acetate in anhydrous acetone for 2 d at –90°C and for 38.9 more hours with gradual temperature increase (6°C/h to −20°C over 11.7 h, constant temperature at −20°C for 16 h, and 10°C/h to 20°C over 4 h). The fixed animals were embedded in araldite resin following the infiltration series (30% araldite/acetone for 4 h, 70% araldite/acetone for 5 h, 90% araldite/acetone overnight, and pure araldite for 8 h). Mutant and control blocks were blinded. Ribbons of ultra-thin (33-nm) serial sections were collected using an Ultracut 6 microtome (Leica) at the level of the anterior reflex of the gonad. Images were obtained on an electron microscope (H-7100; Hitachi) using a digital camera (Gatan). 250 ultra-thin contiguous sections were cut, and the ventral nerve cord was reconstructed from two animals representing each genotype. Image analysis was performed using ImageJ software. The numbers of synaptic vesicles (~30 nm), dense-core vesicles (~40 nm), and large vesicles (>40 nm) in each synapse were counted and their distance from presynaptic specialization and plasma membrane as well as the diameter of each were measured from acetylcholine neurons VA and VB and the GABA neuron VD. A synapse was defined as the serial sections containing a dense projection as well as sections on either side of that density, which contain synaptic vesicle numbers above the mean number of synaptic vesicles per profile.

Electrophysiology

C. elegans were grown at room temperature (22–24°C) on agar plates with a layer of OP50 *Escherichia coli*. Adult hermaphrodite animals were used for electrophysiological analysis. Miniature and evoked postsynaptic currents (mPSCs and ePSCs) at the neuromuscular junction were recorded as previously described (Liu et al., 2007) using a technique originally developed by Richmond and Jorgensen (1999). In brief, an animal was immobilized on a sylgard-coated glass coverslip by applying a cyanoacrylate adhesive along the dorsal side. A longitudinal incision was made in the dorsolateral region. After clearing the viscera, the cuticle flap was folded back and glued to the coverslip, exposing the ventral nerve cord and two adjacent muscle quadrants. A microscope (Axioskop; Carl Zeiss, Inc.) equipped with a 40× water immersion lens and 15× eyepieces was used for viewing the preparation. Borosilicate glass pipettes with a tip resistance of ~3–5 MΩ were used as electrodes for voltage clamping. The classical whole-cell configuration was obtained by rupturing the patch membrane of a gigaohm seal formed between the recording electrode and a body wall muscle cell. The cell was voltage clamped at −60 mV to record mPSCs and ePSCs. ePSCs were evoked by applying a 0.5-ms square wave current pulse at a supramaximal voltage (25 V) through a stimulation electrode placed in close apposition to the ventral nerve cord. Postsynaptic currents were amplified (EP10; HEKA) and acquired with Patchmaster software (HEKA). Data were sampled at a rate of 10 kHz after filtering at 2 kHz. The recording pipette solution contained the following: 120 mM KCl, 20 mM KOH, 5 mM TES, 0.25 mM $CaCl_2$, 4 mM MgCl2, 36 mM sucrose, 5 mM EGTA, and 4 mM Na_2ATP; pH adjusted to 7.2 with KOH and osmolarity at ~310–320 mosM. The standard external solution included the following: 150 mM NaCl, 5 mM KCl, 5 mM $CaCl_2$, 1 mM $MgCl_2$, 5 mM sucrose, 10 mM glucose, and 15 mM Hepes; pH adjusted to 7.35 with NaOH with osmolarity ~330–340 mosM.

Amplitude and frequency of mPSCs were analyzed using MiniAnalysis (Synaptosoft). A detection threshold of 10 pA was used in initial automatic analysis, followed by visual inspections to include missed events (≥5 pA) and to exclude false events resulting from baseline fluctuations. Amplitudes of ePSCs were measured with Fitmaster (HEKA). The amplitude of the largest peak of ePSCs from each experiment was used for statistical analysis. Data were imported into Origin, version 7.5 (OriginLab), for graphing and statistical analysis. Unpaired *t* test was used for statistical comparisons. A value of $P < 0.05$ is considered statistically significant. All values are expressed as mean ± SEM. *n* is the number of worms that were recorded.

Quantification

ImageJ 1.36b was used for the pixel intensity analysis of α adaptin Western blot.

Online supplemental material

Fig. S1 shows rescue of the *apm-2* mutant phenotype. Fig. S2 shows that APM-2 is not mislocalized in endocytic mutants. Fig. S3 shows *apm-2* aldicarb assay. Fig. S4 is a cartoon structure of *apm-2::GFP* DNA constructs. Fig. S5 depicts the assembly of AP2 with or without µ2. Online supplemental material is available at http://www.jcb.org/cgi/content/full/jcb.200806088/DC1.

We thank Barth Grant for kindly providing the APA-2 polyclonal antibody and coelomocyte mRFP::APA-2 strain. We also thank Ken Sato for providing CHC::GFP constructs and GABA neuron GFP::APA-2 strain. We thank Jim Rand and Kiely Grundahl for sharing unpublished information about *unc-41*.

This research was supported by National Institutes of Health grants 5R37NS034307-14 (to E.M. Jorgensen) and NS32057 (to G. Garriga). E.M. Jorgensen is a Howard Hughes Medical Institute Investigator.

Submitted: 13 June 2008
Accepted: 30 October 2008

References

Aguilar, R.C., H. Ohno, K.W. Roche, and J.S. Bonifacino. 1997. Functional domain mapping of the clathrin-associated adaptor medium chains mu1 and mu2. *J. Biol. Chem.* 272:27160–27166.

Augustine, G.J., J.R. Morgan, C.A. Villalba-Galea, S. Jin, K. Prasad, and E.M. Lafer. 2006. Clathrin and synaptic vesicle endocytosis: studies at the squid giant synapse. *Biochem. Soc. Trans.* 34:68–72.

Bao, H., R.W. Daniels, G.T. MacLeod, M.P. Charlton, H.L. Atwood, and B. Zhang. 2005. AP180 maintains the distribution of synaptic and vesicle proteins in the nerve terminal and indirectly regulates the efficacy of Ca2+-triggered exocytosis. *J. Neurophysiol.* 94:1888–1903.

Collins, B.M., A.J. McCoy, H.M. Kent, P.R. Evans, and D.J. Owen. 2002. Molecular architecture and functional model of the endocytic AP2 complex. *Cell.* 109:523–535.

De Camilli, P., K. Takei, and P.S. McPherson. 1995. The function of dynamin in endocytosis. *Curr. Opin. Neurobiol.* 5:559–565.

Dell'Angelica, E.C., J. Klumperman, W. Stoorvogel, and J.S. Bonifacino. 1998. Association of the AP-3 adaptor complex with clathrin. *Science.* 280:431–434.

Dell'Angelica, E.C., C. Mullins, and J.S. Bonifacino. 1999. AP-4, a novel protein complex related to clathrin adaptors. *J. Biol. Chem.* 274:7278–7285.

Dwyer, N.D., C.E. Adler, J.G. Crump, N.D. L'Etoile, and C.I. Bargmann. 2001. Polarized dendritic transport and the AP-1 mu1 clathrin adaptor UNC-101 localize odorant receptors to olfactory cilia. *Neuron.* 31:277–287.

Fergestad, T., and K. Broadie. 2001. Interaction of stoned and synaptotagmin in synaptic vesicle endocytosis. *J. Neurosci.* 21:1218–1227.

Gaidarov, I., and J.H. Keen. 1999. Phosphoinositide–AP-2 interactions required for targeting to plasma membrane clathrin-coated pits. *J. Cell Biol.* 146:755–764.

Gonzalez-Gaitan, M., and H. Jackle. 1997. Role of *Drosophila* alpha-adaptin in presynaptic vesicle recycling. *Cell.* 88:767–776.

Granseth, B., B. Odermatt, S.J. Royle, and L. Lagnado. 2006. Clathrin-mediated endocytosis is the dominant mechanism of vesicle retrieval at hippocampal synapses. *Neuron.* 51:773–786.

Grant, B., and D. Hirsh. 1999. Receptor-mediated endocytosis in the *Caenorhabditis elegans* oocyte. *Mol. Biol. Cell.* 10:4311–4326.

Hammarlund, M., M.T. Palfreyman, S. Watanabe, S. Olsen, and E.M. Jorgensen. 2007. Open syntaxin docks synaptic vesicles. *PLoS Biol.* 5:e198.

Harris, T.W., E. Hartwieg, H.R. Horvitz, and E.M. Jorgensen. 2000. Mutations in synaptojanin disrupt synaptic vesicle recycling. *J. Cell Biol.* 150:589–600.

Haucke, V., M.R. Wenk, E.R. Chapman, K. Farsad, and P. De Camilli. 2000. Dual interaction of synaptotagmin with mu2- and alpha-adaptin facilitates clathrin-coated pit nucleation. *EMBO J.* 19:6011–6019.

Heuser, J.E., and T.S. Reese. 1973. Evidence for recycling of synaptic vesicle membrane during transmitter release at the frog neuromuscular junction. *J. Cell Biol.* 57:315–344.

Honing, S., D. Ricotta, M. Krauss, K. Spate, B. Spolaore, A. Motley, M. Robinson, C. Robinson, V. Haucke, and D.J. Owen. 2005. Phosphatidylinositol-(4,5)-bisphosphate regulates sorting signal recognition by the clathrin-associated adaptor complex AP2. *Mol. Cell.* 18:519–531.

Jorgensen, E.M., E. Hartwieg, K. Schuske, M.L. Nonet, Y. Jin, and H.R. Horvitz. 1995. Defective recycling of synaptic vesicles in synaptotagmin mutants of *Caenorhabditis elegans*. *Nature.* 378:196–199.

Keen, J.H. 1987. Clathrin assembly proteins: affinity purification and a model for coat assembly. *J. Cell Biol.* 105:1989–1998.

Lee, J., G.D. Jongeward, and P.W. Sternberg. 1994. unc-101, a gene required for many aspects of *Caenorhabditis elegans* development and behavior, encodes a clathrin-associatd protein. *Genes Dev.* 8:60–73.

Lewin, D.A., and I. Mellman. 1998. Sorting out adaptors. *Biochim. Biophys. Acta.* 1401:129–145.

Liu, Q., B. Chen, Q. Ge, and Z.W. Wang. 2007. Presynaptic Ca2+/calmodulin-dependent protein kinase II modulates neurotransmitter release by activating BK channels at *Caenorhabditis elegans* neuromuscular junction. *J. Neurosci.* 27:10404–10413.

Mahaffey, D.T., J.S. Peeler, F.M. Brodsky, and R.G. Anderson. 1990. Clathrin-coated pits contain an integral membrane protein that binds the AP-2 subunit with high affinity. *J. Biol. Chem.* 265:16514–16520.

Martina, J.A., C.J. Bonangelino, R.C. Aguilar, and J.S. Bonifacino. 2001. Stonin 2: an adaptor-like protein that interacts with components of the endocytic machinery. *J. Cell Biol.* 153:1111–1120.

Matsui, W., and T. Kirchhausen. 1990. Stabilization of clathrin coats by the core of the clathrin-associated protein complex AP-2. *Biochemistry.* 29:10791–10798.

Maycox, P.R., E. Link, A. Reetz, S.A. Morris, and R. Jahn. 1992. Clathrin-coated vesicles in nervous tissue are involved primarily in synaptic vesicle recycling. *J. Cell Biol.* 118:1379–1388.

Motley, A., N.A. Bright, M.N. Seaman, and M.S. Robinson. 2003. Clathrin-mediated endocytosis in AP-2–depleted cells. *J. Cell Biol.* 162:909–918.

Newton, A.J., T. Kirchhausen, and V.N. Murthy. 2006. Inhibition of dynamin completely blocks compensatory synaptic vesicle endocytosis. *Proc. Natl. Acad. Sci. USA.* 103:17955–17960.

Nguyen, M., A. Alfonso, C.D. Johnson, and J.B. Rand. 1995. *Caenorhabditis elegans* mutants resistant to inhibitors of acetylcholinesterase. *Genetics.* 140:527–535.

Nonet, M.L., A.M. Holgado, F. Brewer, C.J. Serpe, B.A. Norbeck, J. Holleran, L. Wei, E. Hartwieg, E.M. Jorgensen, and A. Alfonso. 1999. UNC-11, a *Caenorhabditis elegans* AP180 homologue, regulates the size and protein composition of synaptic vesicles. *Mol. Biol. Cell.* 10:2343–2360.

Ohno, H., J. Stewart, M.C. Fournier, H. Bosshart, I. Rhee, S. Miyatake, T. Saito, A. Gallusser, T. Kirchhausen, and J.S. Bonifacino. 1995. Interaction of tyrosine-based sorting signals with clathrin-associated proteins. *Science.* 269:1872–1875.

Owen, D.J., and P.R. Evans. 1998. A structural explanation for the recognition of tyrosine-based endocytotic signals. *Science.* 282:1327–1332.

Pan, C.L., P.D. Baum, M. Gu, E.M. Jorgensen, S.G. Clark, and G. Garriga. 2008. *C. elegans* AP-2 and retromer control Wnt signaling by regulating mig-14/Wntless. *Dev. Cell.* 14:132–139.

Phan, H.L., J.A. Finlay, D.S. Chu, P.K. Tan, T. Kirchhausen, and G.S. Payne. 1994. The *Saccharomyces cerevisiae* APS1 gene encodes a homolog of the small subunit of the mammalian clathrin AP-1 complex: evidence for functional interaction with clathrin at the Golgi complex. *EMBO J.* 13:1706–1717.

Richmond, J.E., and E.M. Jorgensen. 1999. One GABA and two acetylcholine receptors function at the *C. elegans* neuromuscular junction. *Nat. Neurosci.* 2:791–797.

Robinson, M.S. 2004. Adaptable adaptors for coated vesicles. *Trends Cell Biol.* 14:167–174.

Robinson, M.S., and J.S. Bonifacino. 2001. Adaptor-related proteins. *Curr. Opin. Cell Biol.* 13:444–453.

Rohde, G., D. Wenzel, and V. Haucke. 2002. A phosphatidylinositol (4,5)-bisphosphate binding site within μ2-adaptin regulates clathrin-mediated endocytosis. *J. Cell Biol.* 158:209–214.

Schuske, K.R., J.E. Richmond, D.S. Matthies, W.S. Davis, S. Runz, D.A. Rube, A.M. van der Bliek, and E.M. Jorgensen. 2003. Endophilin is required for synaptic vesicle endocytosis by localizing synaptojanin. *Neuron.* 40:749–762.

Schuske, K., M.T. Palfreyman, S. Watanabe, and E.M. Jorgensen. 2007. UNC-46 is required for trafficking of the vesicular GABA transporter. *Nat. Neurosci.* 10:846–853.

Shim, J., and J. Lee. 2000. Molecular genetic analysis of apm-2 and aps-2, genes encoding the medium and small chains of the AP-2 clathrin-associated protein complex in the nematode *Caenorhabditis elegans*. *Mol. Cells.* 10:309–316.

Simpson, F., A.A. Peden, L. Christopoulou, and M.S. Robinson. 1997. Characterization of the adaptor-related protein complex, AP-3. *J. Cell Biol.* 137:835–845.

Traub, L.M. 2003. Sorting it out: AP-2 and alternate clathrin adaptors in endocytic cargo selection. *J. Cell Biol.* 163:203–208.

Verstreken, P., O. Kjaerulff, T.E. Lloyd, R. Atkinson, Y. Zhou, I.A. Meinertzhagen, and H.J. Bellen. 2002. Endophilin mutations block clathrin-mediated endocytosis but not neurotransmitter release. *Cell.* 109:101–112.

Verstreken, P., T.W. Koh, K.L. Schulze, R.G. Zhai, P.R. Hiesinger, Y. Zhou, S.Q. Mehta, Y. Cao, J. Roos, and H.J. Bellen. 2003. Synaptojanin is recruited by endophilin to promote synaptic vesicle uncoating. *Neuron.* 40:733–748.

Walther, K., M.K. Diril, N. Jung, and V. Haucke. 2004. Functional dissection of the interactions of stonin 2 with the adaptor complex AP-2 and synaptotagmin. *Proc. Natl. Acad. Sci. USA.* 101:964–969.

Zhang, B., Y.H. Koh, R.B. Beckstead, V. Budnik, B. Ganetzky, and H.J. Bellen. 1998. Synaptic vesicle size and number are regulated by a clathrin adaptor protein required for endocytosis. *Neuron.* 21:1465–1475.

Zhang, J.Z., B.A. Davletov, T.C. Sudhof, and R.G. Anderson. 1994. Synaptotagmin I is a high affinity receptor for clathrin AP-2: implications for membrane recycling. *Cell.* 78:751–760.

Published December 1, 2008

Supplemental Material

JCB

Gu et al., http://www.jcb.org/cgi/content/full/jcb.200806088/DC1

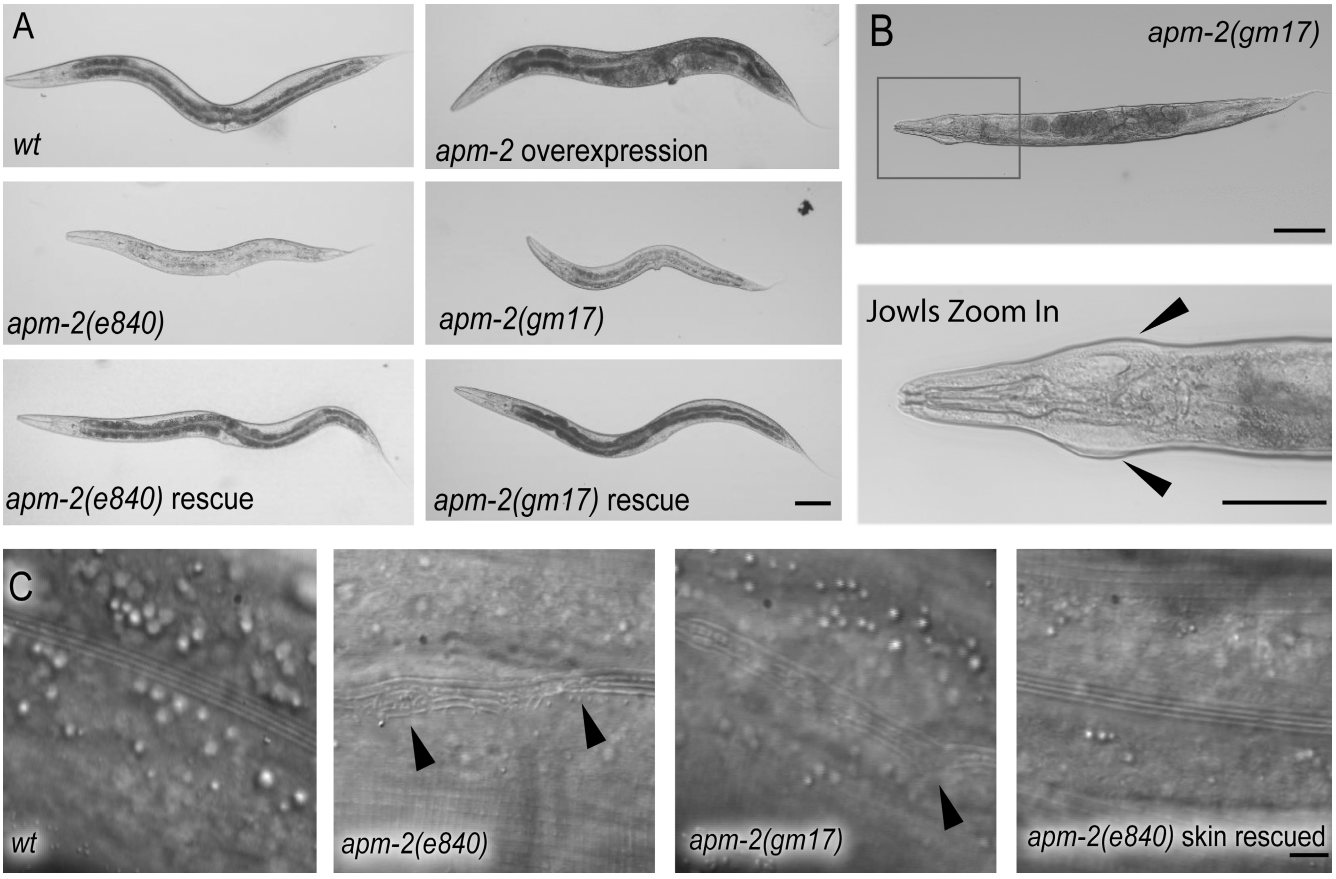

Figure S1. **Rescue of the *apm-2* mutant phenotype.** (A) Bright field images of various *apm-2* genotypes are shown. For the wild type with overexpressed APM-2, the *apm-2* DNA was injected at 10 ng/µl; for *apm-2(e840)* and *apm-2(gm17)* rescued worms, the *apm-2* DNA was injected at 0.25 ng/µl. Bar, 100 µm. (B) Jowls phenotype of *apm-2* mutants. An *apm-2(gm17)* adult hermaphrodite (top) and enlargement of head of the same animal (bottom). Arrowheads indicate jowls. Bars, 100 µm. (C) Alae are cuticular ridges along the sides of animals. Both *apm-2* alleles exhibit breaks or buckles in the alae (arrowheads). The mosaic *apm-2(e840)* strain expressing APM-2::GFP in just the skin is rescued for breaks in the alae. Strain and genotype of skin-rescued strain: EG4029 *apm-2(e840)X; oxEx753[Ppdi-2::APM-2(cDNA)::GFP (pMG8) Punc-122::GFP]*. Bar, 5 µm.

Published December 1, 2008

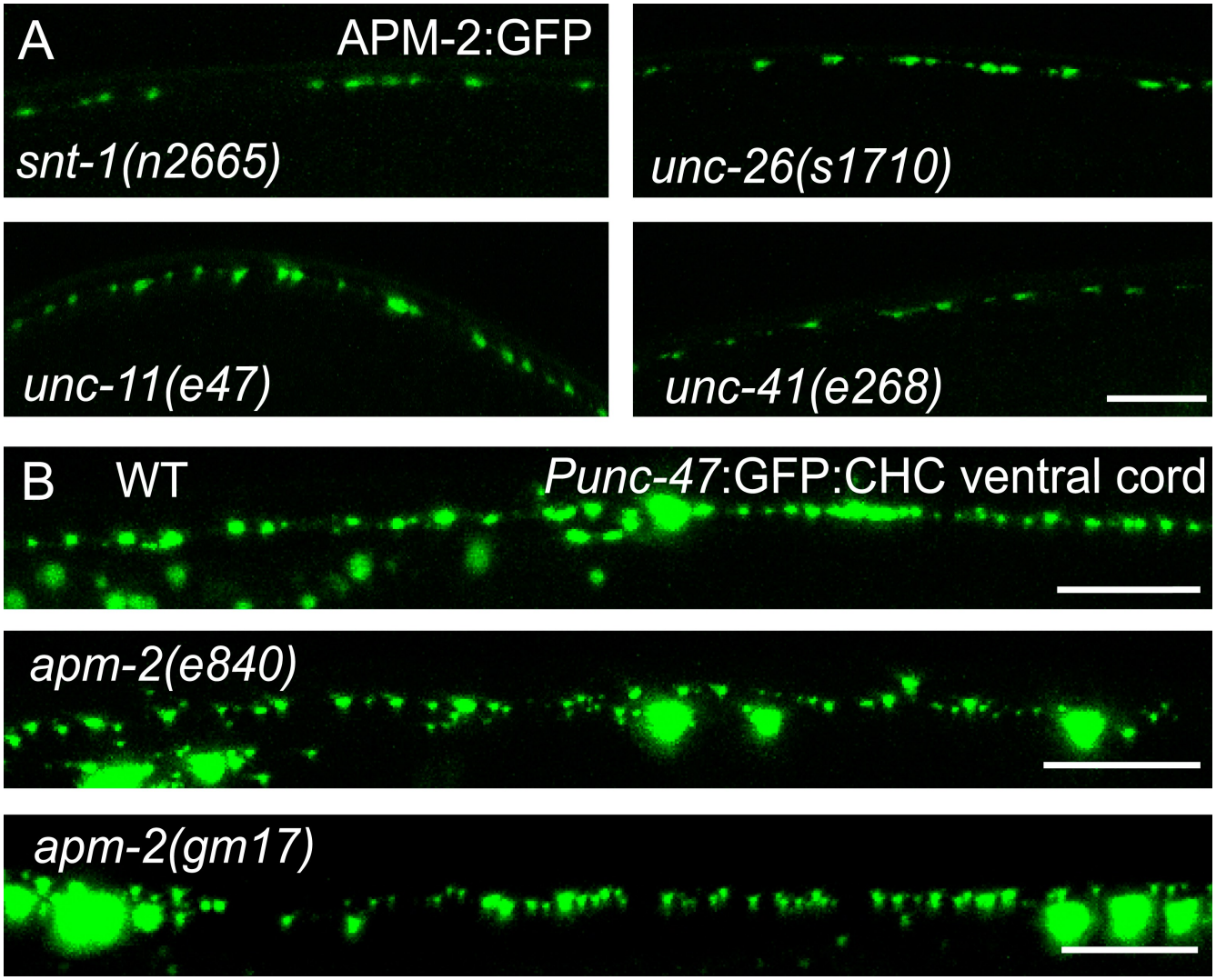

Figure S2. **APM-2 is not mislocalized in endocytic mutants.** (A) APM-2::GFP in the dorsal nerve cord of GABA neurons in *snt-1(n2665)*, *unc-11(e47)*, *unc-26(s1710)*, and *unc-41(e268)* animals. All of these mutants exhibit defects in endocytosis in *C. elegans* (Jorgensen, E.M., E. Hartwieg, K. Schuske, M.L. Nonet, Y. Jin, and H.R. Horvitz. 1995. *Nature.* 378:196–199; Zhang, B., Y.H. Koh, R.B. Beckstead, V. Budnik, B. Ganetzky, and H.J. Bellen. 1998. *Neuron.* 21:1465–1475; Nonet, M.L., A.M. Holgado, F. Brewer, C.J. Serpe, B.A. Norbeck, J. Holleran, L. Wei, E. Hartwieg, E.M. Jorgensen, and A. Alfonso. 1999. *Mol. Biol. Cell.* 10:2343–2360; Harris, T.W., E. Hartwieg, H.R. Horvitz, and E.M. Jorgensen. 2000. *J. Cell Biol.* 150:589–600; Martina, J.A., C.J. Bonangelino, R.C. Aguilar, and J.S. Bonifacino. 2001. *J. Cell Biol.* 153:1111–1120). The fluorescent punctas correspond to synaptic varicosities along the dorsal muscles. (B) Clathrin heavy chain exhibits a punctate distribution in the ventral nerve cords of GABA neurons in both wild-type (EG3381 *oxIs164[Punc-47::GFP::CHC-1 lin-15(+)]IV; lin-15(n765)X*) and *apm-2* animals (EG3735 *oxIs164[Punc-47:GFP::CHC-1 lin-15(+)]IV; apm-2(e840)X* and EG3564 *oxIs164[Punc-47::GFP::CHC-1 lin-15(+)]IV; apm-2(gm17)X*). The large fluorescent spots are the cell bodies of neurons. Bars, 10 μm.

Published December 1, 2008

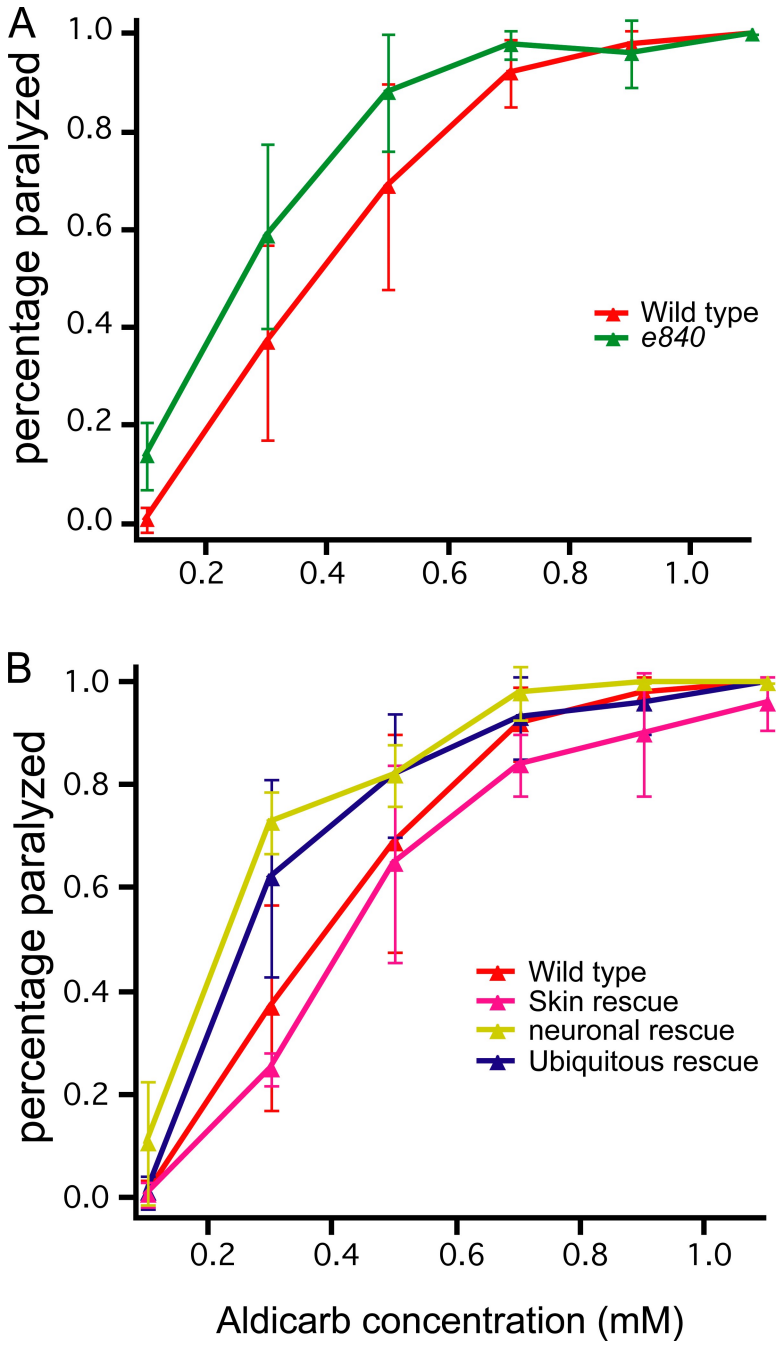

Figure S3. **Aldicarb sensitivity.** Percentage of adult animals paralyzed at given concentration after 4 h. (A) *apm-2(e840)* is aldicarb hypersensitive at 0.1 mM ($P < 0.01$), but it is not significantly different from wild type at other concentrations. (B) Aldicarb sensitivity of *apm-2(e840)* tissue-specific rescued animals. Ubiquitous and skin rescued animals are not significantly different from the wild type. Neuronal rescued animals are aldicarb hypersensitive at 0.3 mM ($P < 0.05$), but are not significantly different from wild type at other concentrations. For each genotype, 100 animals were tested at each concentration, except for neuronal rescue for which only 40 animals were tested at each concentration because of the paucity of transgenic animals. Values are expressed as mean ± SEM.

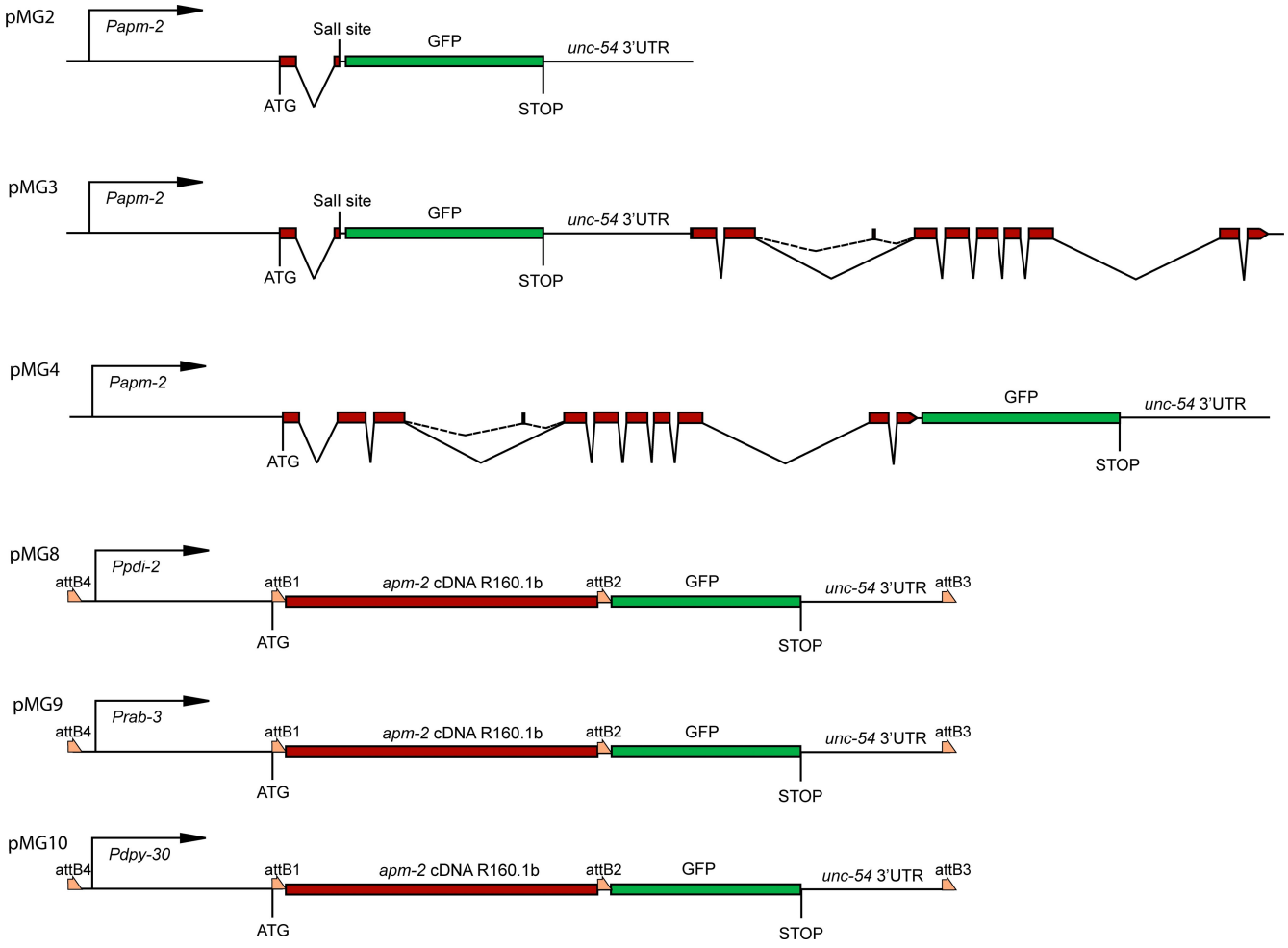

Figure S4. **Cartoon structure of *apm-2::GFP* DNA constructs.**

Published December 1, 2008

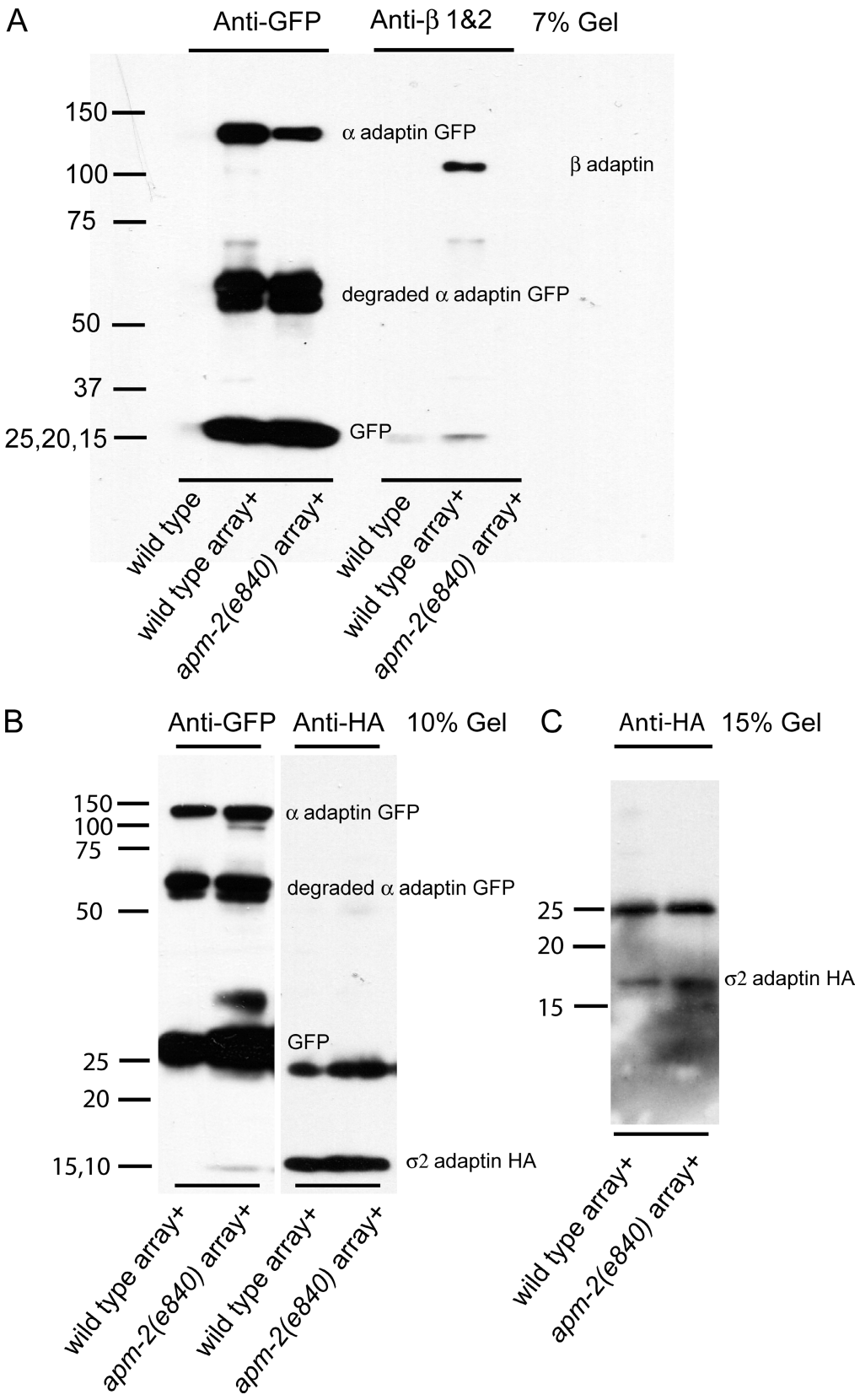

Figure S5. **Assembly of AP2 with or without μ2.** (A) Agarose beads conjugated with rat anti-GFP IgG2a were used to pull down APA-2::GFP from the worm lysate (strain carries array *oxEx1275[Papa-2::APA-2::GFP; Punc-122::GFP]*.). The presence of APA-2::GFP and APB-1 from the pull-down samples were tested by Western blot. The failure to pull down β adaptin in the *apm-2* mutants was confirmed in four blots, from injections of the APA-2::GFP transgene at 1 and 10 ng/μl. (B) Agarose beads conjugated with rat anti-GFP IgG2a were used to pull down APA-2::GFP from the worm lysate (strain carries array *oxEx1276[Papa-2::APA-2::GFP; Paps-2::APS-2::HA; Punc-122::GFP]*.). The presence of APA-2::GFP and APS-2::HA from the pull-down samples was tested by Western blot. (C) The molecular mass of APS-2::HA could not be resolved from 10% SDS-PAGE in B. The same samples were run again in 15% SDS-PAGE and blotted with anti-HA mouse IgG2b.